NASA/TM–2014-218528
NESC-RP-13-00847

Flight Testing of the Space Launch System (SLS) Adaptive Augmenting Control (AAC) Algorithm on an F/A-18

Cornelius J. Dennehy/NESC and Tannen S. VanZwieten/NESC
Langley Research Center, Hampton, Virginia

Curtis E. Hanson
Armstrong Flight Research Center, Edwards Air Force Base, California

John H. Wall
Jacobs Technology, Huntsville, Alabama

Chris J. Miller
Armstrong Flight Research Center, Edwards Air Force Base, California

Eric T. Gilligan
Marshall Space Flight Center, Huntsville, Alabama

Jeb S. Orr
Jacobs Technology, Huntsville, Alabama

September 2014

NASA STI Program . . . in Profile

Since its founding, NASA has been dedicated to the advancement of aeronautics and space science. The NASA scientific and technical information (STI) program plays a key part in helping NASA maintain this important role.

The NASA STI program operates under the auspices of the Agency Chief Information Officer. It collects, organizes, provides for archiving, and disseminates NASA's STI. The NASA STI program provides access to the NASA Aeronautics and Space Database and its public interface, the NASA Technical Report Server, thus providing one of the largest collections of aeronautical and space science STI in the world. Results are published in both non-NASA channels and by NASA in the NASA STI Report Series, which includes the following report types:

- TECHNICAL PUBLICATION. Reports of completed research or a major significant phase of research that present the results of NASA Programs and include extensive data or theoretical analysis. Includes compilations of significant scientific and technical data and information deemed to be of continuing reference value. NASA counterpart of peer-reviewed formal professional papers, but having less stringent limitations on manuscript length and extent of graphic presentations.
- TECHNICAL MEMORANDUM. Scientific and technical findings that are preliminary or of specialized interest, e.g., quick release reports, working papers, and bibliographies that contain minimal annotation. Does not contain extensive analysis.
- CONTRACTOR REPORT. Scientific and technical findings by NASA-sponsored contractors and grantees.
- CONFERENCE PUBLICATION. Collected papers from scientific and technical conferences, symposia, seminars, or other meetings sponsored or co-sponsored by NASA.
- SPECIAL PUBLICATION. Scientific, technical, or historical information from NASA programs, projects, and missions, often concerned with subjects having substantial public interest.
- TECHNICAL TRANSLATION. English-language translations of foreign scientific and technical material pertinent to NASA's mission.

Specialized services also include organizing and publishing research results, distributing specialized research announcements and feeds, providing information desk and personal search support, and enabling data exchange services.

For more information about the NASA STI program, see the following:

- Access the NASA STI program home page at *http://www.sti.nasa.gov*
- E-mail your question to help@sti.nasa.gov
- Fax your question to the NASA STI Information Desk at 443-757-5803
- Phone the NASA STI Information Desk at 443-757-5802
- Write to:
  STI Information Desk
  NASA Center for AeroSpace Information
  7115 Standard Drive
  Hanover, MD 21076-1320

NASA/TM–2014-218528
NESC-RP-13-00847

Flight Testing of the Space Launch System (SLS) Adaptive Augmenting Control (AAC) Algorithm on an F/A-18

Cornelius J. Dennehy/NESC and Tannen S. VanZwieten/NESC
Langley Research Center, Hampton, Virginia

Curtis E. Hanson
Armstrong Flight Research Center, Edwards Air Force Base, California

John H. Wall
Jacobs Technology, Huntsville, Alabama

Chris J. Miller
Armstrong Flight Research Center, Edwards Air Force Base, California

Eric T. Gilligan
Marshall Space Flight Center, Huntsville, Alabama

Jeb S. Orr
Jacobs Technology, Huntsville, Alabama

National Aeronautics and
Space Administration

Langley Research Center
Hampton, Virginia 23681-2199

September 2014

Acknowledgments

In addition to the aforementioned team members, the authors would like to extend appreciation to those who have supported the initial and continued development of the AAC algorithm. This includes Mark Whorton, former Guidance, Navigation, and Mission Analysis Branch Chief at MSFC, for casting the vision and guiding the initial research toward the development of adaptive control for launch vehicles; the late David L. Mellen, Honeywell X-15 Project Engineer, who laid an early vision for forward gain adaptive control and whose published work helped to form the current structure of the SLS AAC technology; and Charles Hall, SLS GN&C lead at MSFC, who has been critical in advocating the maturation and inclusion of AAC, when appropriate, as part of the SLS baseline autopilot design. Several other members of the NASA community also served key roles in allocating time during the algorithm's initial development phase, providing expert review, gaining support within the NASA community, and obtaining resources toward the flight characterization experiment, including MSFC line managers Don Krupp, Mark Jackson, Stephen Ryan, and David Edwards, as well as SLS managers and engineers Jimmy Compton, Jiann-Woei (Jimmy) Jang, John Hanson, Mark West, and Garry Lyles.

The team would like to thank engineers Nhan Nguyen at Ames Research Center (ARC), Irene Gregory at Langley Research Center (LaRC), and John Bosworth and John Burken at Armstrong Flight Research Center (AFRC) for participating in the peer review of the flight experiment. The support of David Voracek, AFRC Chief Technologist, is also appreciated for providing resources that allowed AFRC engineers to complete the initial advocacy and the final reporting of the experiment.

The team is also grateful for the funding partnership between the NESC and the SLS Program, AFRC Technical Excellence, and the STMD GCDP, toward the completion of this flight campaign.

Available from:

NASA Center for AeroSpace Information
7115 Standard Drive
Hanover, MD 21076-1320
443-757-5802

Flight Testing of the Space Launch System (SLS) Adaptive Augmenting Control (AAC) Algorithm on an F/A-18

Volume 1

July 31, 2014

Report Approval and Revision History

NOTE: This document was approved at the July 31, 2014, NRB. This document was submitted to the NESC Director on August 28, 2014, for configuration control.

Approved:	*Original Signature on File*	8/29/14
	NESC Director	Date

Version	Description of Revision	Office of Primary Responsibility	Effective Date
1.0	Initial Release	Mr. Cornelius J. Dennehy, NASA Technical Fellow for GN&C, GSFC	7/31/14

Table of Contents

Technical Assessment Report

List of Figures

List of Tables

Technical Assessment Report

1.0 Notification and Authorization

The Marshall Space Flight Center (MSFC) Flight Mechanics and Analysis Division developed an adaptive augmenting control (AAC) algorithm for launch vehicles that improves robustness and performance on an as-needed basis by adapting a classical control algorithm to unexpected environments or variations in vehicle dynamics. This was baselined as part of the Space Launch System (SLS) flight control system. The NASA Engineering and Safety Center (NESC) was asked to partner with the SLS Program and the Space Technology Mission Directorate (STMD) Game Changing Development Program (GCDP) to flight test the AAC algorithm on a manned aircraft that can achieve a high level of dynamic similarity to a launch vehicle and raise the technology readiness of the algorithm early in the program.

Mr. Cornelius J. Dennehy, NASA Technical Fellow for Guidance, Navigation, and Control (GN&C), was selected as the NESC lead, with Dr. Tannen VanZwieten assigned as the technical lead. The assessment plan was approved by the NESC Review Board (NRB) on January 17, 2013.

The key stakeholders for this assessment were Mr. Garry Lyles, SLS Program Chief Engineer; Mr. Kurt Jackson, SLS Program Integrated Avionics and Software Discipline Lead Engineer; and Mr. Mark West, SLS Vehicle Management Discipline Lead Engineer.

2.0 Signature Page

Submitted by:

Team Signature Page on File - 9/11/14

Mr. Cornelius J. Dennehy Date

Significant Contributors:

Dr. Tannen S. VanZwieten Date	Mr. Curtis E. Hanson Date
Mr. John H. Wall Date	Mr. Chris J. Miller Date
Mr. Eric T. Gilligan Date	Dr. Jeb S. Orr Date

Signatories declare the findings, observations, and NESC recommendations compiled in the report are factually based from data extracted from program/project documents, contractor reports, and open literature, and/or generated from independently conducted tests, analyses, and inspections.

3.0 Team List

Name	Discipline	Organization
Core Team		
Neil Dennehy	NESC Lead	GSFC
Tannen VanZwieten	Technical Lead (Controls)	MSFC
Chris Miller	F/A-18 Test Chief Engineer	AFRC
Patricia Pahlavani	MTSO Program Analyst	LaRC
Flight Test Support		
Curtis Hanson	Controls	AFRC
James Lee	F/A-18 Test Chief Engineer (Retired)	AFRC
Oscar Murillo	Controls	AFRC
Richard Larson	Systems Lead	AFRC
Dan Goodrick	Instrumentation Lead	AFRC
Richard Weaver	Safety	AFRC
James Less	Pilot	AFRC
David Larson	Pilot	AFRC
Brian Griffin	Operations Lead	AFRC
William Fredricksen	Avionics Lead	AFRC
Otis Allen	Avionics	AFRC
Donald Warren	Crew Chief	AFRC
Donald Herman	Mechanic	AFRC
Marlin Picket	Simulation Lead	AFRC
Karla Shy	Control Room	AFRC
John Carter	Project Manager	AFRC
John Kelly	Project Manager	AFRC
Scott Erickson	Quality Assurance	AFRC
Bob Perry	Program Analyst	AFRC
SLS Algorithm Development		
Eric Gilligan	Algorithm Development	MSFC
Jeb Orr	Algorithm Development	MSFC/The Charles Stark Draper Laboratory
John Wall	Algorithm Development	MSFC/Dynamic Concepts
Consultants		
Victoria Regenie	NESC Systems Engineering Office	AFRC
Kenneth Lebsock	NESC GN&C Technical Discipline Deputy Lead	GSFC/Orbital Sciences
Daniel Murri	NASA Technical Fellow for Flight Mechanics	LARC
James Stewart	NESC Chief Engineer at AFRC	AFRC

Name	Discipline	Organization
Steven Gentz	NESC Chief Engineer at MSFC	MSFC
Don Krupp	Control Systems Design and Analysis Branch Chief	MSFC
Charles Hall	SLS GN&C Lead	MSFC
Steve Derry	Controls/PTI Waveform Development	LaRC
Administrative Support		
Linda Burgess	Planning and Control Analyst	LaRC/AMA
Jonay Campbell	Technical Writer	LaRC/NG
Pamela Sparks	Project Coordinator	LaRC/AMA

3.1 Acknowledgements

In addition to the aforementioned team members, the authors would like to extend appreciation to those who have supported the initial and continued development of the AAC algorithm. This includes Mark Whorton, former Guidance, Navigation, and Mission Analysis Branch Chief at MSFC, for casting the vision and guiding the initial research toward the development of adaptive control for launch vehicles; the late David L. Mellen, Honeywell X-15 Project Engineer, who laid an early vision for forward gain adaptive control and whose published work helped to form the current structure of the SLS AAC technology; and Charles Hall, SLS GN&C lead at MSFC, who has been critical in advocating the maturation and inclusion of AAC, when appropriate, as part of the SLS baseline autopilot design. Several other members of the NASA community also served key roles in allocating time during the algorithm's initial development phase, providing expert review, gaining support within the NASA community, and obtaining resources toward the flight characterization experiment, including MSFC line managers Don Krupp, Mark Jackson, Stephen Ryan, and David Edwards, as well as SLS managers and engineers Jimmy Compton, Jiann-Woei (Jimmy) Jang, John Hanson, Mark West, and Garry Lyles.

The team would like to thank engineers Nhan Nguyen at Ames Research Center (ARC), Irene Gregory at Langley Research Center (LaRC), and John Bosworth and John Burken at Armstrong Flight Research Center (AFRC) for participating in the peer review of the flight experiment. The support of David Voracek, AFRC Chief Technologist, is also appreciated for providing resources that allowed AFRC engineers to complete the initial advocacy and the final reporting of the experiment.

The team is also grateful for the funding partnership between the NESC and the SLS Program, AFRC Technical Excellence, and the STMD GCDP, toward the completion of this flight campaign.

4.0 Executive Summary

The NASA Engineering and Safety Center (NESC) was asked to partner with the Space Launch System (SLS) Program and the Space Technology Mission Directorate's Game Changing Development Program (GCDP) to flight test the SLS adaptive augmenting control (AAC) algorithm on a piloted Fighter/Attack (F/A)-18. The AAC algorithm, developed within the Marshall Space Flight Center (MSFC) Flight Mechanics and Analysis Division, augments the fixed-gain portion of the SLS flight control system (FCS) in order to maximize launch vehicle survivability and crew safety. AAC, also referred to herein as launch vehicle adaptive control (LVAC), was baselined as part of the FCS design but was the only element that had not yet been flight tested.

With the unique capabilities of its Airborne Research Test System (ARTS) and a previously certified nonlinear dynamic inversion (NDI) controller, the F/A-18 Full-Scale Advanced Systems Testbed (FAST) aircraft was able to match the SLS model attitude error dynamics during flight. This capability allowed the SLS FCS, including the AAC component but excluding the disturbance compensation algorithm (DCA), to be applied as the control system for the F/A-18 so that its performance could be demonstrated in a flight environment.

A series of research flights were conducted in November and December of 2013, which verified that the AAC algorithm functionally met its design objectives through multiple SLS scenarios and over a hundred SLS-like trajectories. This included verification of the ability of the SLS FCS to recover from adverse flight conditions using adaptation since many of the simulated flight conditions could not be suitably accommodated in the absence of the adaptive algorithm.

The flight tests also explored interactions between manual steering and the AAC. Although the research flights demonstrated that AAC can aid the vehicle's ability to retain stable flight control and limit flight loads during certain adverse scenarios, the use of AAC as-implemented when manual steering is engaged can increase the probability of an adverse pilot-vehicle interaction. Thus, if a manual steering mode is used in future SLS missions, design changes or fade-out of the adaptive component upon engagement may be needed.

The success of the flight tests prior to the SLS Program's Critical Design Review (CDR) raised the technology readiness level (TRL) of the AAC algorithm to level 7, "System prototype demonstration in an operational environment." This demonstration of AAC also increased internal and external confidence in the algorithm readiness for the first unmanned flight test of the SLS.

This collaborative engineering/flight test effort represented not only a significant contribution to the SLS Program but also aligned with one of the top technical challenges of the guidance, navigation, and control (GN&C) discipline. This challenge is for NASA to investigate and gain hands-on experience with "modern" control theory/methodologies, such as adaptive control, as potential solutions to demanding flight control problems. Therefore, although motivated by a need within the SLS Program, the benefits extend to the NASA GN&C community.

5.0 Assessment Plan

The technical activities planned for this assessment occurred in two phases. The first phase consisted of the algorithm development, integration, and verification, while the second phase consisted of the research flights. The technical team initiated the first phase upon receiving authority to proceed, while completion of the second phase was contingent upon aircraft readiness. The two phases, as well as the key milestones for this assessment and the associated SLS Program design analysis cycles (DACs) and reviews, are shown in Figure 5.0-1.

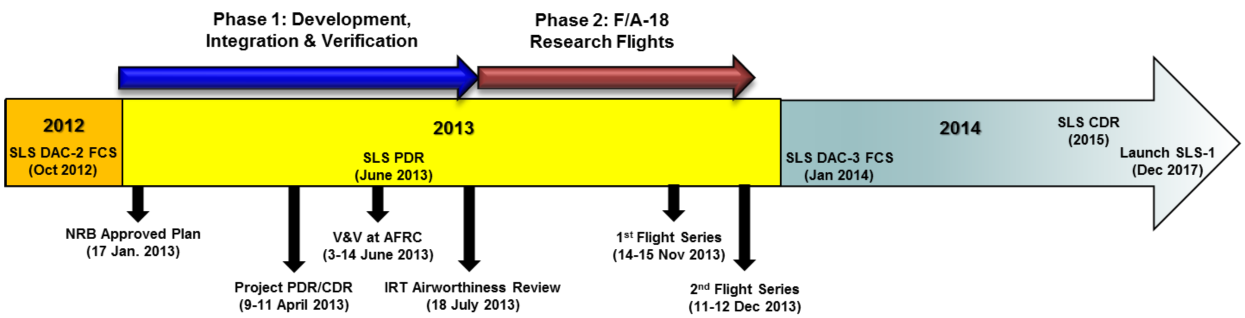

Figure 5.0-1. Key Milestones for Assessment and the SLS Program

The activities completed during each phase were as follows:

Phase 1: Algorithm Development, Integration, and Verification

The following algorithm development activities were accomplished at MSFC and Armstrong Flight Research Center (AFRC) with significant collaboration and integration:

- Modified the SLS FCS for F/A-18 FAST aircraft.
  - Modified the interfaces and deactivated the DCA in baseline SLS FCS, then delivered for integration into the experiment software.
  - Developed experiment-appropriate flight software using the ARTS IV research computer onboard the FAST aircraft, including switching logic to support multiple test cases (TCs).
- Developed SLS reference model and associated TCs and completed FAST NDI modifications.
  - Developed models using the SLS dynamics for use as a reference model in the FAST NDI controller.
  - Developed TCs using near- and off-nominal SLS scenarios.
  - Developed an NDI controller that will achieve the SLS reference model dynamics, both nominal and off-nominal, within the capabilities of the aircraft.
- Defined flight plan/trajectory.
  - Provided a trajectory guidance algorithm design and necessary parameter loads.
- Completed the following reviews:
  - System Requirements Review at AFRC.

  - Technical interchange meeting at MSFC.
  - Independent review team (IRT) joint Preliminary Design Review (PDR)/CDR at AFRC, requests for action (RFAs) from the IRT, and RFA resolutions from the documented IRT Airworthiness Review.
  - Technical brief to the AFRC management to obtain concurrence of airworthiness and a signed flight request officially releasing the team to execute the flights as briefed.
- Documented and prepared flight package for review, including:
  - Objectives and requirements document (ORD) (see Appendix G).
  - Detailed hazard reports analyzing the potential asset and human risks associated with the experiment. Developed at a series of meetings of the System Safety Working Group.
  - Software requirements and design document (SRDD) (see Appendix H).
  - Verification and validation test plan (VVTP) (see Appendix I).
  - Flight test plan (FTP) (see Appendix J).
- Completed verification and validation (V&V).
  - Provided information and/or analysis as required to satisfactorily close IRT RFAs.
  - Conducted V&V testing on the experiment software.
  - Documented the flight media as tested and loaded on the aircraft in the configuration control process addressing any discrepancies from V&V.
- Completed flight preparation.
  - Wrote flight test cards and completed piloted simulation evaluation of all planned test points.
  - Developed and validated control room displays for real-time monitoring.
  - Completed control room training via a real-time simulated mission.
  - Executed a combined systems test to verify proper combined functionality of aircraft research and instrumentation systems, telemetry, and control room displays.

Phase 2: Flight Testing

Six research flights were completed using the SLS FCS. Multiple scenarios were flown, which map into each of the flight objectives described in Section 6.4 with emphasis on performing a functional check of the AAC.

6.0 Background

In-house development of an AAC algorithm for launch vehicles as an addition to the classical control architecture began during the Constellation Program (CxP) [ref. 1]. Development of the adaptive algorithm was accelerated during the SLS Program, where the NASA community has continued to develop confidence in the algorithm through extensive internal and external reviews, stability analysis, flight software implementation and testing, time and frequency-domain analysis of failure scenarios, and Monte Carlo analysis. Maturation of the algorithm coupled with the demonstration of tangible, predictable benefits led to the AAC algorithm being baselined as part of the autopilot design and flight software build prior to the SLS PDR in 2013.

The SLS Block I vehicle (see Figure 6.0-1) will deliver more payload to orbit and produce more thrust than any other foreign or domestic launch vehicle, opening the way to new frontiers of space exploration. Like all large launch vehicles, the SLS must balance the competing needs of maximizing performance while maintaining robustness. With its large size, high thrust, and multiple elements, the SLS is a highly flexible structure with complex bending characteristics. Control commands must be allocated to each of its six engines, which are actuated along the pitch and yaw axes by thrust vector control (TVC) actuators with limited bandwidth. The massive propellant tanks have lightly damped lateral sloshing modes, and the uncertain payload envelope produces a unique set of parasitic dynamics. The SLS trajectories are optimized to maximize performance, which further challenges the flight control design and leaves little margin to share among multiple disciplines and subsystems.

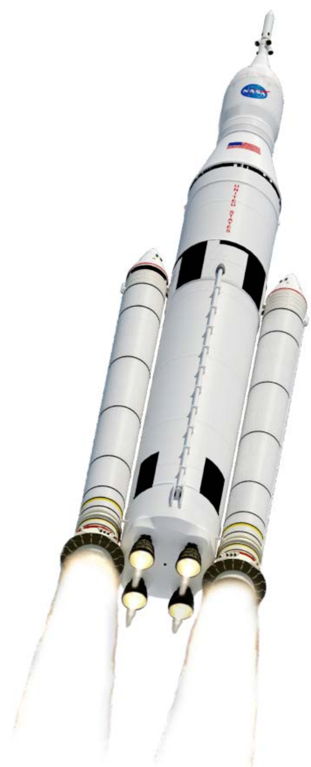

Figure 6.0-1. SLS Block I Vehicle

In the current fast-paced, low-cost development environment, there is a need for new technologies or design innovation to be coupled with affordable, quick-turnaround testing options. Testing the SLS FCS on a small-scale launch vehicle or a sounding rocket would require the SLS software to be tailored to the existing vehicle specifications, including a re-optimization of the control parameters to provide the experimental platform with adequate closed-loop attitude tracking. Furthermore, these platforms lack key features of the SLS dynamics (e.g., low-frequency bending modes), which are needed to evaluate the adaptive law. Implementation on a piloted aircraft became an attractive alternative since AFRC demonstrated the F/A-18 FAST, shown in Figure 6.0-2, as capable of matching the dynamics of a reference model and safely accommodating a variety of control experiments. Furthermore, this testbed aircraft allowed for substantially longer flight times, multiple experiment conditions, and more data collection than the other platforms under consideration. Thus, the tests were conducted using the SLS FCS flight software prototype under SLS-based scenarios as though it was flying the SLS vehicle while hosted on the surrogate F/A-18 platform. Within a year of the concept study, a series of flight experiments was completed in November and December of 2013 on an F/A-18 aircraft, tail number (TN) 853. These flights were a key contributor to the maturation of the AAC technology, the only component of the SLS control architecture lacking flight heritage. The flights represent the completion of an important milestone toward the SLS baseline control design V&V.

Figure 6.0-2. F/A-18 FAST

6.1 Motivation for Advanced Control

The AAC scheme was designed to improve launch vehicle robustness and performance by adapting an otherwise well-tuned classical control algorithm to unexpected environments or variations in vehicle dynamics. The original motivation for considering the development and inclusion of an advanced control approach for human-rated launch vehicles did not result from an inability of the traditional fixed-gain control design to achieve satisfactory performance when the vehicle dynamics and environments were well-characterized. In the absence of vehicle or environmental uncertainty, a fixed-gain controller could be optimized such that there would be no motivation for on-line adaptation. However, a review of historical reusable launch vehicle data from 1990 to 2002 revealed that 41 percent of failures in other subsystems might have been mitigated by advanced GN&C technologies [ref. 2]. Control approaches that use real-time adaptation thrive when there are environmental or vehicle model uncertainties, including in-flight anomalies and failure scenarios. Traditional barriers to capitalizing on the benefits of advanced control techniques that are particularly relevant for human-rated systems include algorithm and code complexity, predictability of the response, ability to reconcile the stability analysis in the context of classical gain and phase margin, and flight certification. In other words, "black box" approaches with numerous adaptive gains, complex nonlinearities, and no way of estimating classical stability margins would be difficult to justify from a risk perspective, even if performance exceeded that of the existing architecture. Thus, an algorithmically simple, predictable AAC design compatible with classical stability margin assessment was implemented for the SLS.

6.2 Overview of the SLS AAC Algorithm

The philosophy that drove the formulation of the AAC algorithm, its initial testing during the CxP [ref. 1], and its refinement as part of the baseline autopilot design for the SLS [refs. 3 and 4] was to maintain nominal system performance and be compatible with classical stability criteria. Thus, an adaptive system was developed with a predictable response that augments the existing control architecture and prefers the nominal control gains. Secondly, the philosophy was to provide additional robustness using a simple architecture that could recover from poor closed-loop performance and prevent or delay loss of mission (LOM) or loss of vehicle (LOV). To effectively accomplish this goal, model reference adaptive control logic was used within the adaptive update law to increase the control gain when excessive tracking error indicates that system performance is less than preflight predictions. An additional adaptive update term was included that decreases the adaptive gain when excessive power within a prescribed frequency band is observed in the control command as a result of control coupling with launch vehicle parasitic dynamics (e.g., flexibility, fuel slosh, and actuators). This gain-decreasing element is a feature that balances the competing objectives of reducing the tracking error while maintaining stability of the plant dynamics not represented in the reference model. Only a subset of adaptive control approaches that appear in the open literature recognize the importance of decreasing performance to recover stability even if the error associated with the primary tracking objective is increasing. Figure 6.2-1 illustrates the as-needed gain adaptation design paradigm for the SLS AAC algorithm.

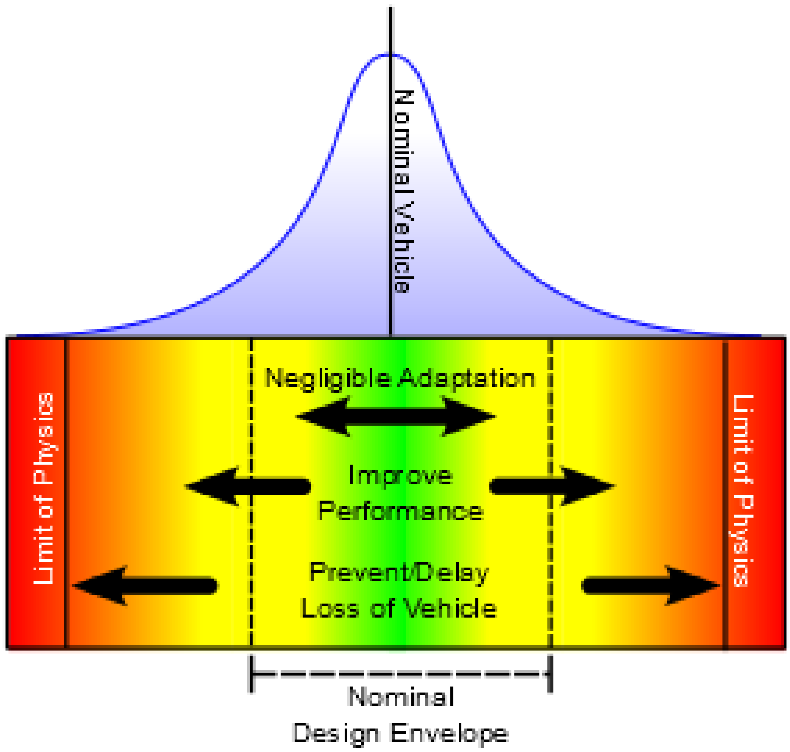

Figure 6.2-1. The AAC Algorithm Design Paradigm is to Adapt on an As-needed Basis

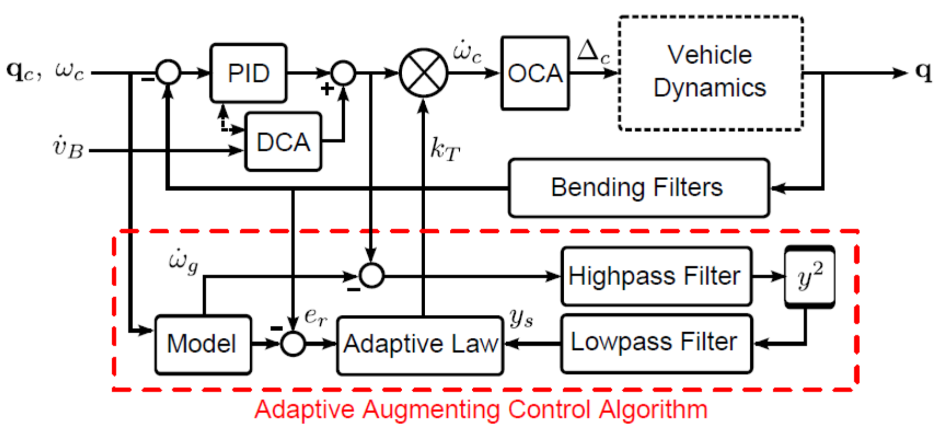

Figure 6.2-2. Block Diagram of the SLS FCS with AAC

The resulting AAC algorithm was a forward loop gain (k_T) multiplicative architecture that modifies the total attitude control system gain in response to sensed model errors (e_r) and undesirable resonance in the control loop (y_s) resulting from control interactions with parasitic modes (see Figure 6.2-2). The AAC alters performance by increasing or decreasing forward loop gain, thereby balancing attitude tracking with the attenuation of undesirable frequency content within the control path. In the case of the latter, this is often due to unmodeled or mismodeled parasitic dynamics that would otherwise result in a closed-loop instability or a potentially destructive limit cycle. In this case, the adaptive controller responds to the frequency content in the control signal by decreasing the total loop gain to reduce the interaction between these dynamics and the controller. The AAC algorithm is computationally simple and has stability properties that are reconcilable in the context of classical frequency-domain criteria. Since FCS guidelines provide a minimum of 6 decibels (dB) of rigid body margin and 6 dB of aero margin for the nominal vehicle, limits on the adaptive gain are restricted accordingly with a minimum value of 0.5 and a maximum value of 2.

In the absence of vehicle or environmental uncertainty, a gain-scheduled controller can be optimized prior to flight, which would eliminate the motivation for adaptation. Adaptive control provides additional robustness by using sensed data to adjust the loop gain in flight. The algorithm was designed under the assumption that the gain-scheduled attitude control design is tuned for a nominal vehicle and trajectory at each flight time (i.e., adaptation should only occur should the vehicle performance lie outside the nominal design envelope), as depicted in Figure 6.2-1. Therefore, by design the adaptive gain is attracted to unity through the use of a modified leakage term. The result is that only small alterations are made to the fixed-gain design within the expected dispersion envelope, without requiring the use of a dead zone in the update law. The AAC characteristics in simulation reflect the algorithm's three summary-level objectives:

1. “Do no harm;” return to baseline control design when not needed.
2. Increase performance; respond to error in ability of vehicle to track commands.
3. Regain stability; respond to undesirable control-structure interaction or other parasitic dynamics.

Note that the AAC was not designed to explicitly alter the ascent trajectory due to a lower performing vehicle (e.g., degraded thrust) or off-nominal environment (e.g., wind bias). Such techniques under the broader study of advanced guidance methods are beyond the scope of the AAC algorithm.

The AAC has been implemented in the SLS MAVERIC and SAVANT 6-degree-of-freedom simulation tools and was baselined for DAC-2. The SLS DAC-2 supplementary Monte Carlo analysis concluded no penalties associated with the algorithm and helped uncover other flight control performance artifacts (e.g., filter transition effects) [ref. 3]. These results and others completed via high-fidelity CxP Ares I and SLS simulations have demonstrated the capability of the AAC to “do no harm” in nominal scenarios, while increasing the attitude control robustness to vehicle and environmental uncertainties and failure scenarios. The result is a decreased likelihood of LOM or an extension in the abort eligibility in the event of a catastrophic event (e.g., case breach). A unique feature of the algorithm is its capability to protect against adverse control structure interaction.

6.3 Motivation for Flight Testing

The AAC algorithm reached a high maturity level as part of the SLS autopilot design through simulation-based development, as well as internal and external reviews. However, leading into the SLS PDR, the AAC remained the only component of the vehicle control system that had not been flight tested. All other dynamic elements of the control system were successfully tested through Ares I-X [refs. 5 and 6]. Completion of the testing described in this paper means that every algorithm in the SLS control design architecture has been successfully demonstrated in flight, as shown in Figure 6.3-1.

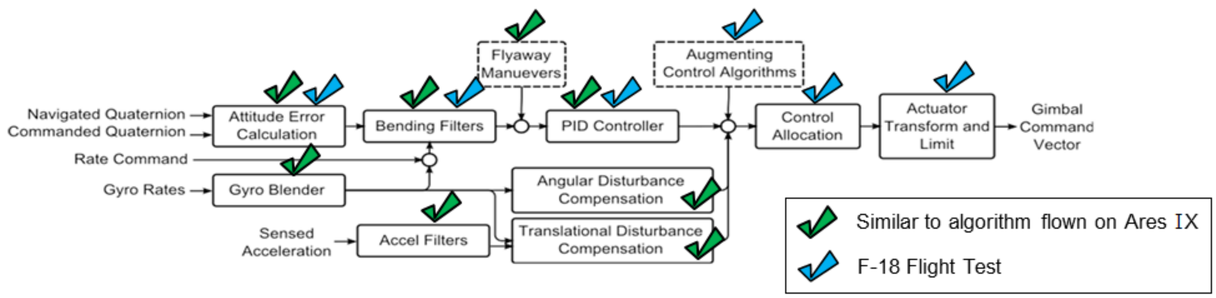

Figure 6.3-1. Flight Testing of the SLS Autopilot Flight Software Prototype

6.3.1 TRL Assessment

One of the major objectives of this investigation was to raise the TRL of the AAC algorithm early in the SLS Program. The determination of an appropriate TRL maturity is not clear for all systems, leaving it somewhat to the discretion of the subject matter experts. However, identification of a system's TRL provides consistent language for communicating the state of a technology across the Agency and should be considered with other factors. For SLS, the increased TRL gained through the research flights is part of a larger scale risk mitigation strategy that includes internal and external review, stability analysis, Monte Carlo simulations, and simulation-based SLS scenarios that exhibit anomalous behavior.

NASA releases two categories under which the TRL of a system or subsystem can be assessed: hardware and software [ref. 7]. While the SLS FCS algorithms are coded into flight software, the software definitions point to a need to repeat a maturation process whenever there is a change in a software build or associated hardware. For the SLS flight software, the MSFC Software Integration Laboratory (SIL) will support the software maturation to TRL 8, but this does not imply that the algorithms will be fully vetted. Furthermore, when evaluating an algorithm's readiness for use on a launch vehicle, it would not be logical to consider flight-tested methods (e.g., the standard architecture with a fixed-gain proportional-integral-derivative (PID) controller and bending filters) to have a low TRL. Taking these perspectives into consideration, the software definitions are mentioned herein, but the AAC algorithm TRL is defined based on the hardware description.

Prior to testing the AAC algorithm through the F/A-18 research flights, the algorithm reached a TRL 5 level of maturity. The algorithm did not meet the TRL 6 criteria since the AAC had not yet been demonstrated in an operational environment. TRL 5 is summarized as "component and/or breadboard validation in a laboratory environment." The associated hardware definition for TRL 5 is as follows [ref. 7]:

> *A medium fidelity system/component brassboard is built and operated to demonstrate overall performance in a simulated operational environment with realistic support elements that demonstrate overall performance in critical areas. Performance predictions are made for subsequent development phases.*

The AAC algorithm was tested in a simulated operational environment. Performance had been demonstrated in critical functional areas through the use of a linear MATLAB®-based model (i.e., medium-fidelity system). Performance was evaluated based on the simulation results.

The software definition associated with TRL 5 was met, defined as follows [ref. 7]:

> *End-to-end software elements implemented and interfaced with existing systems/simulations conforming to target environment. End-to-end software system tested in relevant environment, meeting predicted performance. Operational environment performance predicted. Prototype implementations developed.*

End-to-end GN&C flight software elements have been implemented on multiple simulation environments, including a target computer by the flight software team. Algorithm performance is documented as part of the SLS GN&C performance assessment, which is released each design cycle. Agreement of test performance on the target computer is assessed based on the ability to meet specific metrics.

The F/A-18 research flights increased the AAC's TRL from 5 to 7, based on the hardware definition provided in reference 7. The descriptions and justification for reaching TRL 7, based on the hardware description and TRL 6 for both hardware and software descriptions, is provided in Figures 6.3-2 and 6.3-3, respectively.

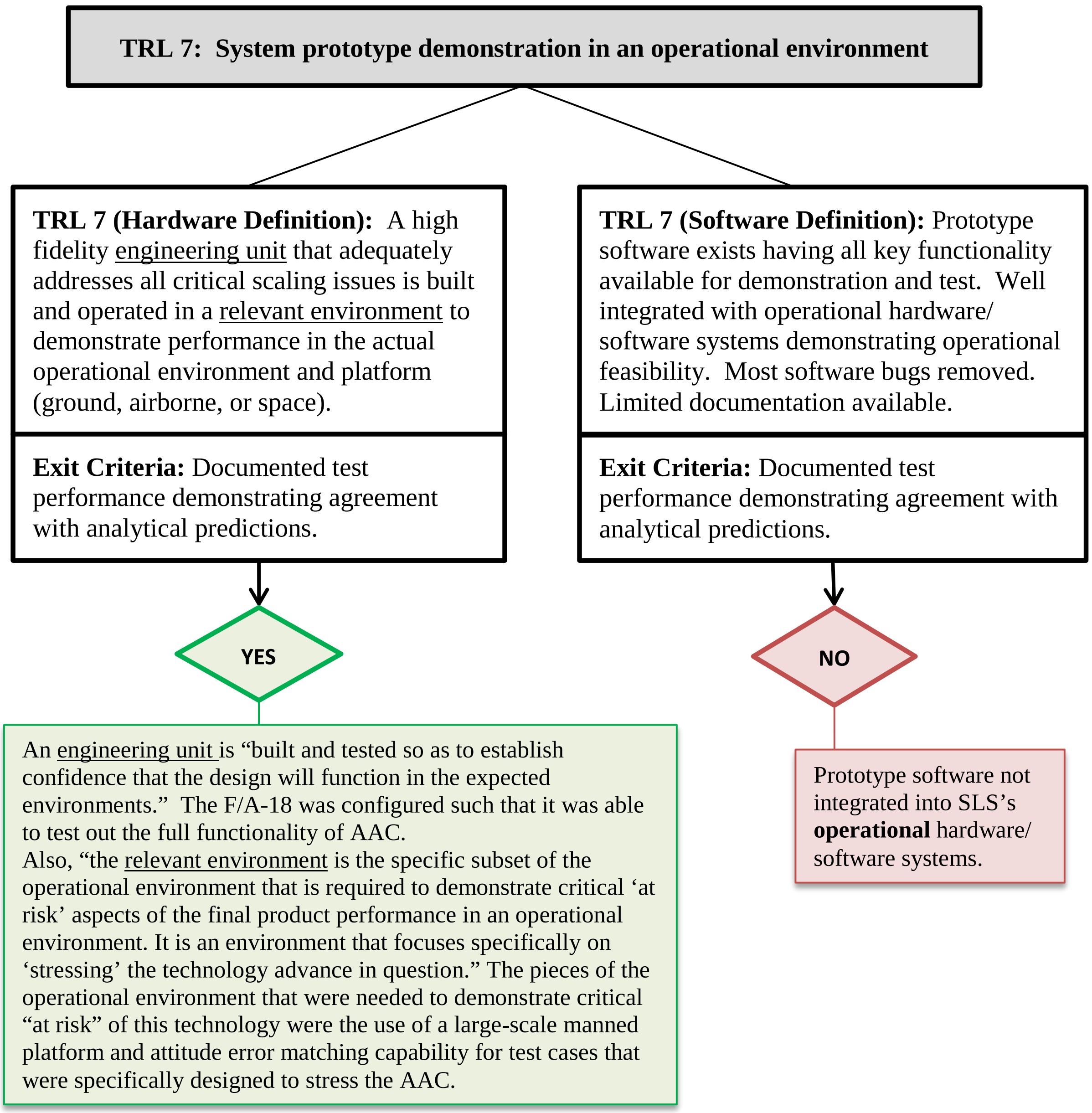

Figure 6.3-2. AAC TRL 7 Justification: After F/A-18 Flights

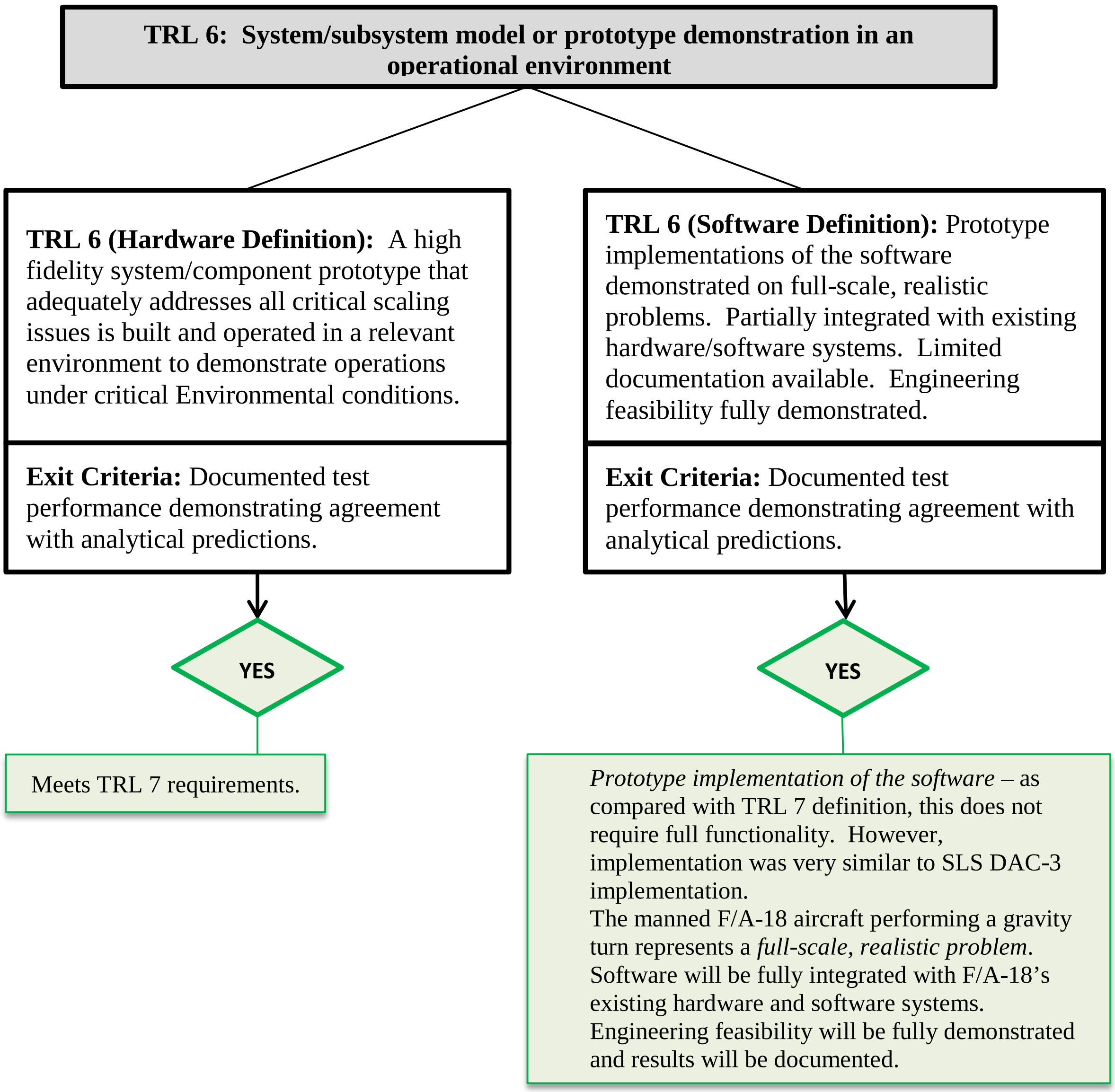

Figure 6.3-3. AAC TRL 6 Justification: After F/A-18 Flights

6.4 Objectives of the Research Flights

The F/A-18 FAST was used as a platform for conducting a flight characterization experiment intended to validate that the AAC algorithm achieves the purposes for which it was designed. Additionally, in consideration of the SLS requirement to incorporate manual steering capability that existed at the time this study was initiated, it is desirable to understand the pilot/ACC interaction. Thus, the primary objectives of the research flights are summarized as follows:

1. Demonstrate closed-loop tracking with negligible adaptation in an environment that is commensurate with the nominal controller design envelope.
2. Demonstrate improved performance in an environment where the nominal controller performance is less than desired.
3. Demonstrate the ability to recover from unstable, mismodeled parasitic dynamics to a bounded nondestructive limit cycle.
4. Explore interactions between manual steering and the AAC.

The approach for achieving these objectives was to develop multiple SLS scenarios that consider physically realizable normal and failure conditions that map into objectives 1 through 3. An additional TC was developed to demonstrate objective 3 by staging control-structure interaction with the physical resonance of the F/A-18 airframe. To achieve objective 4, a subset of these scenarios was repeated with the pilot providing attitude commands.

Additional design considerations to enhance the value of the results were to maximize the dynamic similarity between the aircraft and SLS pitch attitude error dynamics, incorporate as much of the SLS FCS as possible to capture its interactions with the AAC, and force the AAC to respond to a physical realization of unfavorable SLS dynamics rather than cancelling high-frequency motion inside the aircraft's software package when possible. The experiment development process was structured to allow the SLS controls engineers to gain valuable insight toward the software integration and flight certification of the full-scale algorithm. In addition to validating the AAC in conjunction with the fixed-gain portion of the FCS, the process of developing TCs in the MSFC simulation environment, testing each of them in the F/A-18 hardware-in-the-loop simulation (HILS), and then capturing flight test results allowed for verification that the flight software performed as expected.

7.0 Construction of Dynamically Relevant Research Flights

Combining the value of testing the AAC in a relevant environment with the need for an affordable testing option led to the unconventional approach of conducting simulated launch vehicle flight tests on a research aircraft. Control experiments have been supported previously on AFRC's F/A-18, but this is the first time the aircraft was considered for testing an algorithm specifically designed and tuned for launch vehicles. To aid in understanding the relevance of the test results, this section provides an overview of the aircraft platform and key features of the implementation for the launch vehicle flight experiment. The following sections do not capture every detail of the implementation but are intended to illustrate at a basic level the relevant aspects of the test platform and implementation for the launch vehicle experiment.

7.1 Applicability of the F/A-18 as an SLS Flight Test Platform

This flight characterization experiment was performed on the F/A-18 (TN 853) FAST platform [ref. 8]. This aircraft is maintained by AFRC and was developed specifically to accommodate a variety of controls experiments with full command authority of the F/A-18 and its available control surfaces. Aided by the presence of a qualified research pilot, the F/A-18 TN 853 has an experimental envelope called the Class B envelope that is defined by altitude and Mach constraints (Figure 7.1-1). Constraining experiments within this envelope ensures safe recovery from unusual attitudes and configurations. The favorable recoverability characteristics and the structural robustness of the aircraft while inside the Class B envelope allowed AFRC engineers to pre-clear the aircraft for full-authority experimental control while inside the prescribed altitude and Mach constraints. The aircraft features production and research sensor inputs, pilot experiment engage/disengage capability, real-time configuration of multiple experiments on a single flight, as well as failure detection with automatic reversion to the fail-safe production mode. As with the traditional FCS, the experimental controller inside the Class B envelope is able to control ten aerodynamic effectors and two throttles.

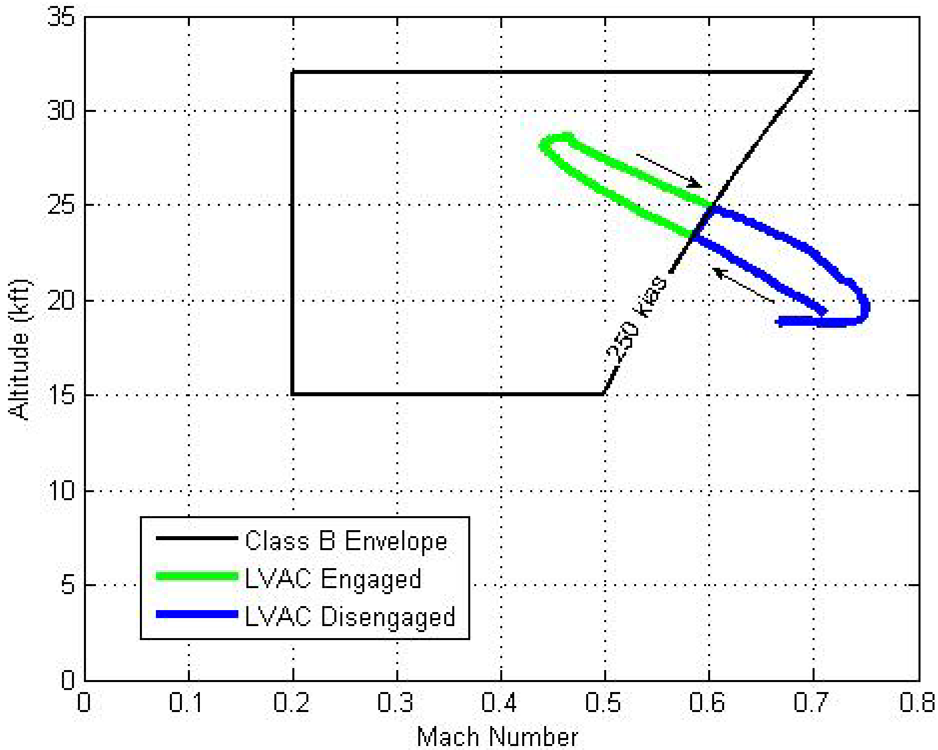

Figure 7.1-1. Class B Envelope and Sample Trajectory

The idea that an F/A-18 can represent a relevant environment for the purpose of advancing the TRL of an adaptive control technique for the SLS vehicle is novel and requires an in-depth explanation. The FAST F/A-18 was not the only candidate considered for testing. The other platform options will not be discussed in this section, as the intent is to explain the key features of the FAST vehicle that make it a relevant test platform.

The first key to performing a meaningful test on the F/A-18 is that the aircraft has sufficient performance, even when restricted to the class B research envelope, to fly a near-ballistic trajectory, which is a reasonable approximation of the SLS gravity turn boost trajectory. The shape of the pitch rate command for the F/A-18 zoom climb and subsequent near-ballistic trajectory was designed to be similar to that of the SLS to solid rocket booster (SRB) separation. More details of the trajectory can be found in Section 7.2. An illustration of the trajectory projected onto the Class B envelope restrictions (i.e., altitude and Mach ranges) is shown in Figure 7.1-1.

In addition to the command shape similarity provided by the zoom climb trajectory, another important aspect of dynamic similarity is matching the rigid body attitude dynamics along that trajectory. Matching the SLS attitude dynamics was accomplished by the F/A-18 inner loop NDI controller, which forced the aircraft to exhibit the angular acceleration response of a given plant model. As a result, the responses of the F/A-18 pitch angle error, pitch rate, and pitch acceleration were nearly the same as predicted for the SLS vehicle and could be used as inputs to its FCS. In this way, the SLS FCS “thinks it is flying SLS” when it is engaged on the near-ballistic F/A-18 trajectory. In addition to matching the SLS rigid body pitch dynamics, the NDI provided the FAST vehicle with the ability to track other aspects of the SLS (e.g., simulated atmospheric disturbances), parasitic dynamics (e.g., structural modes), and various failure modes. This inner loop controller is described in greater detail in Section 7.3 and in Appendix F.

The SLS performance, combined with the dynamic similarity, resulted in a test trajectory of approximately 70 seconds. This represents a sufficiently large portion of the SLS boost trajectory, such that the time scaling of the adaptive controller during the F/A-18 tests can directly match the time scaling for the SLS vehicle. This feature allows for verification of the adaptation rates, gains, and architecture, requiring minimal changes to the flight configuration SLS controller.

The flexibility of the research flight control computers on the FAST vehicle allowed accommodation of software from various sources and programing languages. These flight computers, combined with the SLS-like trajectories, suitable flight times, and the NDI, allowed for hosting of the flight prototype C and C++ SLS control laws on the F/A-18. This capability allowed the team to test for software errors using AFRC’s F/A-18 HILS and during the research flights. As a result, software findings during the preparation or execution of the LVAC research flights were corrected in the SLS prototype flight software.

Additionally, the FAST platform, with the ability to remove the production F/A-18 structural filters and excite the existing structural modes, provided a test scenario for the adaptive controller to respond to a physical, rather than a modeled, airframe structural mode. While the F/A-18 first fuselage mode was at higher frequency than the lowest frequency SLS structural modes that typically drive the control design, the aircraft fuselage mode was in the range typically analyzed by the SLS Controls Working Group during each SLS design cycle. Due to the structural robustness and limited dynamic pressure (*q*) within the Class B envelope, preflight analysis showed that the aircraft mode could be excited through the use of a programmed test input (PTI) and an intentionally destabilizing FCS design with negligible risk of aircraft damage. This provided the LVAC experiment with an ideal test scenario for evaluating the AAC response to a structural mode in a safe but relevant way. The F/A-18 structural mode was more highly damped than the expected SLS modes in the same frequency range, which has implications on the frequency of the resulting stable limit cycles when the AAC was activated but does not negate the value of the test involving this mode.

The presence of a test pilot and the ability to drive pilot cueing displays allowed for the testing of the interactions between a manual steering mode and the adaptive controller. This test objective was of lower priority, but provided an environment to explore manual steering implementation. The test uncovered important deficiencies that will need to be addressed if manual steering is required, and if manual steering is used in combination with the AAC on the SLS. It is important to note that the manual steering mode evaluated during this experiment was not the official SLS manual steering mode design or implementation, as an official design did not yet exist.

Finally, the nature of the FAST architecture allowed for an array of test scenarios during a single mission and allowed the researchers to reconfigure the experiment between flights with minimal recertification testing. This rapid prototyping capability, combined with the ability to repeatedly test numerous SLS-based scenarios in rapid succession, made the platform not only relevant with respect to the stated flight test objectives, but attractive from a cost and schedule perspective.

Other options (e.g., sounding rockets) were explored, but testing the first three AAC objectives would not have been possible due to the limited number and configurability of the tests within the same budget constraints. Furthermore, this option would not provide the test times and repeatability offered by the FAST platform. While other NASA test assets (e.g., AirSTAR) could provide similar computational and software integration capabilities, the tests would have been performed at faster time scales, which may have required extensive scaling computations and analysis to justify the utility of the test results. The FAST platform offered more test and longer maneuver times than a single rocket or missile test, thereby providing increased opportunity to fully and repeatedly exercise many aspects of the algorithm. Finally, the use of a manned vehicle required that the experiment development process be reconciled with appropriate safety and risk mitigation requirements, thus enhancing the applicability of both the tested algorithm/software package and the experience of the development team on the operational platform.

7.1.1 Description of the F/A-18 FAST Platform

FAST is a single-seat F/A-18 aircraft, as shown in Figures 7.1-2 and 7.1-3. Substantial research instrumentation (e.g., structural, air data, and inertial) has been installed to support a wide range of research activities. The robust nature of the testbed (i.e., structural load capacity, spin and recovery characteristics, and reversion to production control laws), with the research instrumentation, enabled flight testing of novel control laws on a piloted flight vehicle with minimal validation testing requirements.

Figure 7.1-2. F/A-18 in Flight

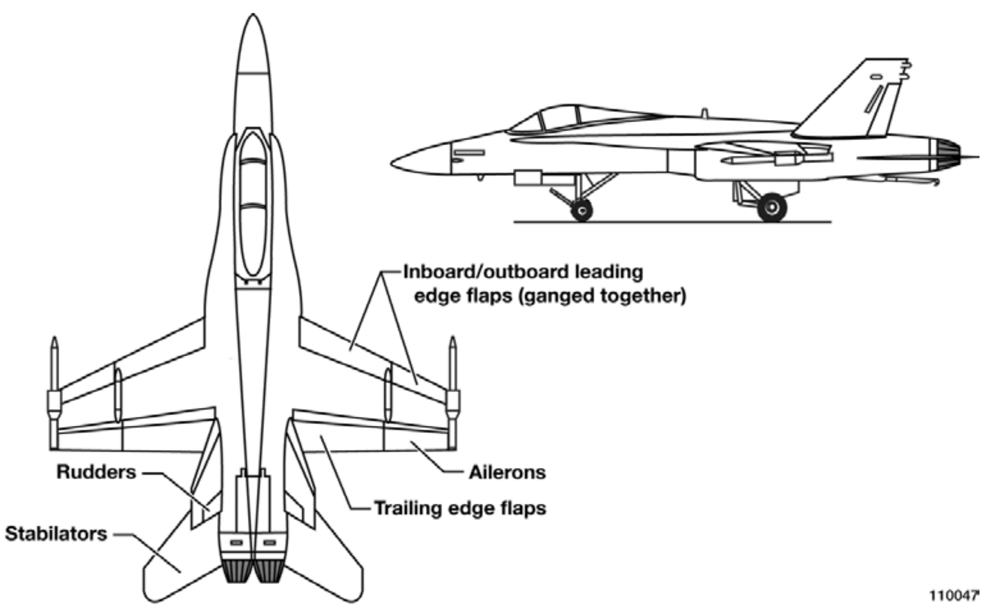

Figure 7.1-3. F/A-18 Profile

Figure 7.1-4 shows the FAST control computer and system architecture. The system maintains the advantages of the production system and utilizes its redundancy management architecture for sensor selection and actuator signal management. The FAST research flight control computer architecture, which builds upon legacy F/A-18 research systems, consists of two separate research processing capabilities. The research flight control system (RFCS) provides a minimal delay quad-redundant processing environment in which Ada-programmed experiments can be executed. The RFCS performs some protection for restricting the engagement envelope of a given research control law hosted in either the ARTS or the RFCS (see Figure 7.1-1). The ARTS, with its more capable processor and the ability to host Simulink® autocode or C code, provides a more flexible environment for novel control laws than the RFCS. However, the ARTS is only dual-redundant and imparts one additional frame of delay to commands. This extra frame of delay translated to 0.0125 seconds for the pitch and roll axes and 0.025 seconds for the yaw axis.

The LVAC experiment took advantage of the ample computation and data storage capabilities in the ARTS, as well as the autocoding capability supported via a MATLAB®/Simulink® model-based design environment. The flight software prototype of the SLS autopilot, already coded in C, was also hosted within the ARTS.

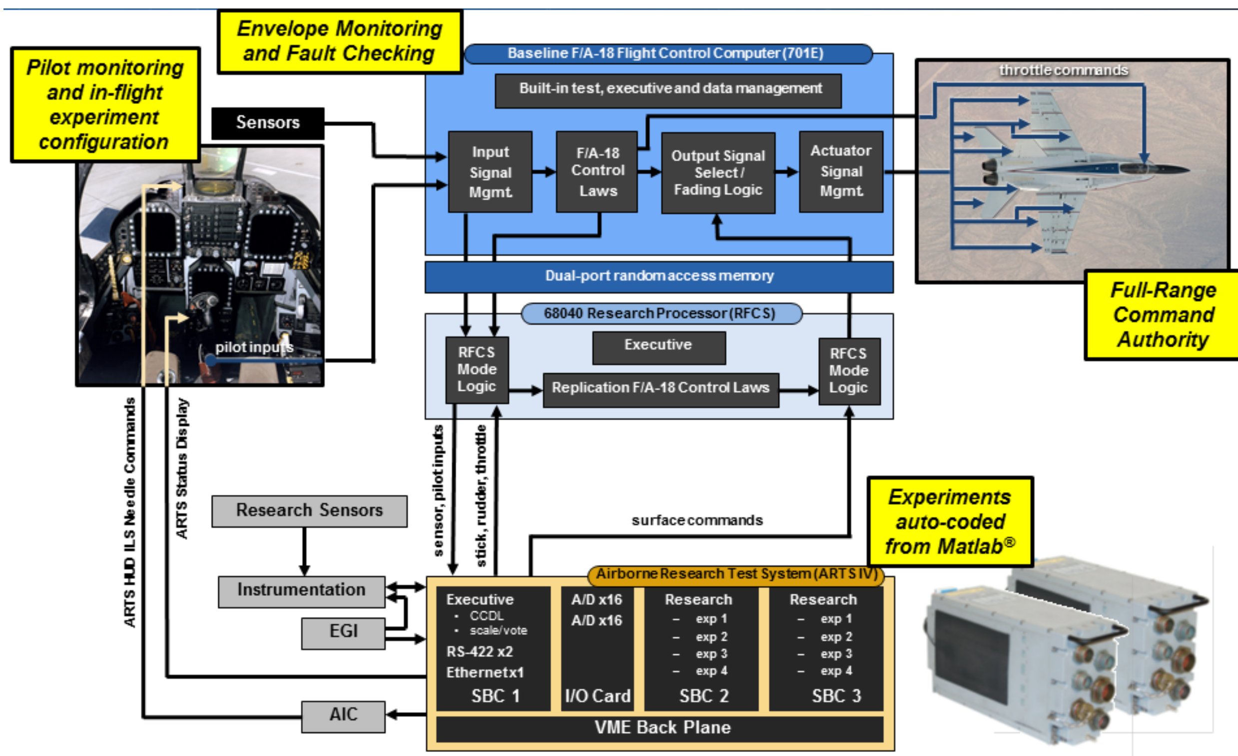

Figure 7.1-4. RFCS/ARTS

Additionally, the FAST research system was designed to provide the experimenter with the flexibility to configure the experiment in flight through the use of selectable parameters that are entered by the pilot. As configured for LVAC, the FAST aircraft was able to support up to 221 unique TC scenarios. Any of these scenarios that have been configured and appropriately verified prior to flight could be engaged as the active experiment configuration during a flight test mission. This provides the researcher with a great deal of flexibility when designing and testing cutting-edge control technologies, and facilitates highly effective research missions. For the LVAC experiment, this array of configurable options was essential due to the limited number of sorties and the flight schedule, which was compounded by the large number of TCs desired to verify the ACC design objectives.

The ability to provide command cueing to the pilot from an ARTS experiment is a new capability that was added to the FAST vehicle specifically for the LVAC manual steering objective. Experimenters now have the ability to provide a visual command reference to the pilot using the production instrument landing system (ILS) display on the FAST vehicle from a research experiment hosted on the ARTS. This feature allows researchers to design maneuvers for the human pilot and quantitatively explore how well the pilot is able to track the trajectories for a wide range of control configurations and simulated failure scenarios. This is a valuable capability for experimenters exploring the interaction of a pilot with the control technique.

Lastly, the FAST system includes communication with the aircraft research instrumentation system. This capability allows for utilization of many research instrumentation measurements as closed-loop control law feedback sensors. This feature expands the types of control architectures and novel sensor experiments that can be facilitated by the platform. For the LVAC experiment, this capability was utilized to explore how the AAC algorithm performed with two different pitch rate sensors installed at separate locations on the aircraft to amplify the physical F/A-18 airframe structural response in the control path.

7.2 Experiment Trajectory

The aircraft's trajectory was designed to track a pitch rate of approximately 0.75 degree/second, which was used as an input to the SLS FCS during the experiment in lieu of SLS' outer-loop guidance commands. This rate is near the average pitch rate of the SLS during its gravity turn prior to SRB separation. During project formulation, an exact zero-g (gravity) turn was considered as a candidate test trajectory. However, the FAST aircraft is prohibited from sustained zero- and negative-g maneuvers. Additionally, attaining these low-g trajectories required high pitch rates and would have resulted in much shorter test trajectories. The experiment was not designed to match the aircraft's pitch attitude to that of the SLS, since this would require a near-vertical flight path. That profile is not achievable since the aircraft's thrust-to-weight ratio is less than unity at the altitudes at which experiment is flown. The need to perform the experiment inside the Class B envelope further constrained the aircraft trajectory design since initiating the trajectory at a high pitch attitude would result in the aircraft rapidly losing speed and flying out of the envelope, thereby reducing the time available on each trajectory to perform the controls experiment. Thus, the trajectory was designed to provide pitch rates that closely approximate those of the SLS and maximize the experiment time, given the constraints imposed by the Class B envelope. Figure 7.1-1 shows a sample trajectory (blue/green lines) that achieves the desired test time (green line) within the Class B experimental envelope (black lines) during a simulated flight.

A diagram of the resulting trajectory design is shown in Figure 7.2-1, starting with the setup maneuver (blue line) leading to the operation of the SLS FCS (green line). Prior to initiating each test scenario, the pilot accelerated the aircraft to approximately 330 knots (Mach 0.5) and 19,000 ft, and then rotated to 35-degree pitch attitude. This resulted in a decreasing Mach number as the aircraft pitched up and entered the Class B envelope, which needed to occur at a low enough altitude that aircraft did not exceed the maximum altitude constraint at the peak of its trajectory (see Figure 7.1-1). Once at the desired altitude, Mach, and pitch attitude, the pilot armed and engaged the desired SLS experiment. The entrance criteria for the experiment were not exact and had a small impact on the control surface effectiveness and available trajectory time. Thus, the overall repeatability of the experiment results was not significantly impacted by the variability of the maneuver initiation. Furthermore, the pilots were able to achieve the insertion conditions with the precision needed to complete the trajectory within the Mach and altitude constraints prescribed by the Class B envelope for a majority of the attempts (see Appendix A for documentation of complete/incomplete trajectories). After the experiment was engaged, the autopilot tracked the desired pitch rate unless manual steering was engaged. The pilot monitored the experiment and managed aircraft throttle near peak altitude to extend the test time within the Class B velocity envelope as it began its pitch downward. Engine gyroscopic coupling and the aerodynamic disruption of the sudden change in engine inlet flow resulted in a pitch transient due to the de-throttle, but the pilots were able to ensure a smooth, gradual throttle transition, which minimized this undesirable pitch transient and the subsequent effect on the test results.

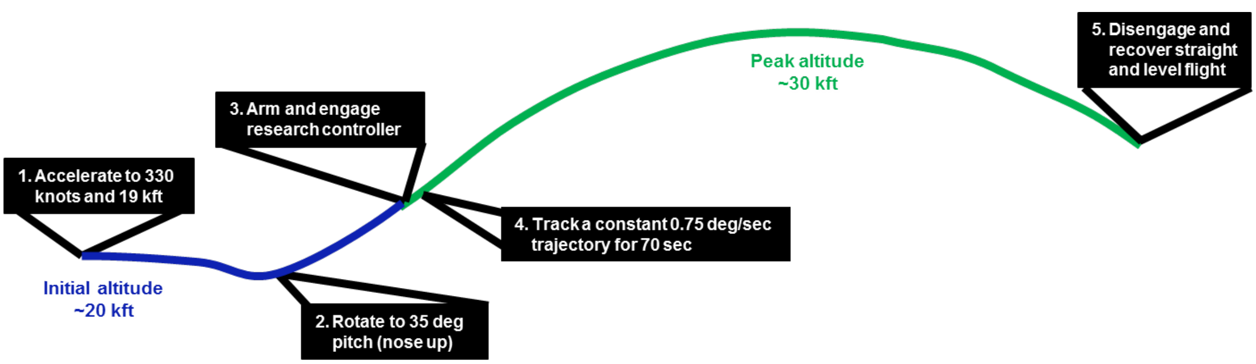

Figure 7.2-1. Prescribed Trajectory for the Flight Experiment

During a typical sortie, between 16 and 29 trajectories approximately matching the one described in Figure 7.2-1 were completed within the available airspace until fuel constraints required the aircraft to land. Each time the trajectory was repeated during flight, the aircraft was configured with a different SLS test scenario. Images taken of FAST performing this trajectory as part of the SLS experiment are shown in Figure 7.2-2. Exceptions to the aforementioned trajectory implementation were for (1) manual steering, where the pilot sought to track the desired attitude rate while performing the experiment, and (2) experiments to detect, excite, and mitigate an airframe structural mode, during which the pilot maintained straight and level flight.

Figure 7.2-2. Photographs Depicting the Trajectory Flown Repeatedly by the F/A-18

7.3 Nonlinear Dynamic Inversion to Achieve Pitch Attitude Matching

A key to the F/A-18 representing a relevant test environment for the AAC technique as it is applied to the SLS autopilot was that the relevant measured dynamics (e.g., pitch error and rate) and control responses of the FAST vehicle had to be made to match those of the SLS vehicle during the boost phase prior to SRB separation. The justification for advancing the ACC TRL in a relevant environment was dependent on the pitch attitude dynamic response matching across a wide range of desired frequencies to the bandwidth limitations of the F/A-18 rigid body and actuator responses.

The NDI baseline control law was developed as part of the FAST suite of research capabilities [refs. 9 and 10]. It has been used on a number of experiments to provide desirable vehicle control response characteristics for the control technique under test. It is based on a simple conservation of angular moment formulation. Given a three-axis desired angular acceleration, the NDI computes the necessary F/A-18 control surface commands required to generate the commanded angular acceleration. The NDI utilizes the F/A-18 aerodynamics with nonlinear rigid body equations of motion to divide out the underlying airframe dynamics and replace them with those of the desired plant.

For the LVAC experiment, the desired plant was that of the SLS vehicle. A planar, high-fidelity SLS simulation using linearized plant dynamics and nonlinear actuator models [ref. 11] was delivered and implemented as the desired dynamics for the FAST vehicle to track. This model (i.e., reference model) runs in the ARTS with the SLS control laws and provides the NDI with reference commands to track. The model contains the relevant dynamics (e.g., structural modes, slosh modes, actuator dynamics, rigid body characteristics, failure modes, environmental disturbances, etc.).

One unique aspect of the LVAC experiment was the requirement to generate different aspects of the vehicle dynamics with the F/A-18 control surfaces. This requirement was driven by the test scenarios involving the SLS vehicle elastic response. For the tests involving structural modes to be of maximum value, a different set of control surfaces is used to generate the simulated SLS structural dynamics on the F/A-18 rigid body from the set of surfaces used to respond to those dynamics. If the same set of surfaces is used for both tasks, then the experiment is effectively generating and canceling out the structural dynamics inside the software, which provides significantly less benefit with regard to flight over a ground simulation. Generating the dynamics with one set of surfaces and then forcing another set to respond to the dynamics generated effectively closes the loop outside the software around the aircraft, significantly increasing the value of the TCs. The NDI was modified from the form used by previous experiments such that the ailerons were used in a symmetrical manner to generate the elastic contribution to the pitch axis dynamics, and the stabilators were used to respond to those dynamics through the simulated SLS vehicle rigid body. The importance of maximizing the value of these simulated structural mode TCs was heightened by the team’s uncertainty about the feasibility of the structural TC utilizing the F/A-18 first fuselage bending mode. Ultimately, both TCs functioned as desired, providing firm confidence in the ACC algorithm TRL.

LVAC test scenarios flown on the F/A-18 were designed using the linear high-fidelity SLS simulation [ref. 11] employing model parameters consistent with the DAC-2. As part of that LVAC simulation, a second-order, time-varying aircraft model was provided by AFRC to account for the NDI and the F/A-18 tracking performance throughout the LVAC trajectory. The resulting scenarios and the SLS model, including plant and controller, were supplied to AFRC, where they were verified in the HILS as part of a formal V&V process. The HILS results matched with the flight data and the MSFC simulation results.

7.4 SLS Reference Dynamics

The LVAC dynamic inversion function reference model was based upon a quasi-linear perturbation flight mechanics formulation derived from a planar, time-varying version of the Frequency Response Analysis and Comparison Tool Assuming Linearity (FRACTAL) model. This model provided the reference states that were duplicated by the F/A-18 pitch response so as to simulate launch vehicle dynamics along the experiment trajectory. FRACTAL is a tool for flight control design and analysis and was derived from the standard modal superposition approach to flexible launch vehicle dynamics [refs. 11 and 12]. This model, within limitations of the planar nature of the simulated flight dynamics, was consistent with the model approach used for the SLS vehicle flight control design.

The LVAC reference dynamics produced a set of reference states as a function of time since trajectory initiation, which was used by the FAST dynamic inversion controller. In general, the rate of change of the reference states is considerably less than the angular acceleration and rate capability of the F/A-18 airframe pitch dynamics. This enabled accurate tracking of the reference model with negligible model error.

During the reference model formulation development, performance limitations in the execution of a simulated launch vehicle ascent profile by an aircraft precluded duplication of a true gravity-turn trajectory. Furthermore, the FAST aircraft trajectory could not duplicate the launch vehicle angle of attack (α) profile through the use of short-period attitude dynamics. This is a key trajectory parameter affecting launch vehicle flight control, which is dependent on air-mass relative velocity. Thus, the LVAC reference model was formulated in such a way that α, crucial for simulating aerodynamically unstable launch vehicle pitch dynamics, was computed using a hybrid scheme. In this manner, a small angle linearization dependent solely on the reference states was replaced by a computation that is dependent on a true kinematic state of the aircraft (i.e., the pitch error) and an internally propagated lateral velocity that simulates the vehicle error velocity with respect to the trajectory. Under the assumption that the reference trajectory is a zero-α trajectory (as is the case for SLS boost-phase flight), the aircraft trajectory-relative pitch error and the internal velocity estimate were combined to compute the internal α.

The LVAC reference formulation included all relevant dynamics associated with the pitch axis of the SLS launch vehicle, including the time-varying rigid-body mass properties, core stage oxidizer and fuel sloshing modes, six bending modes,[1] and nonlinear actuator dynamics associated with each of the six engines (including nozzle inertial coupling effects). Time-varying structural dynamics were implemented using the quadratic inequality constrained least squares (LSQI) transition method [refs. 13 and 14]. The top-level organization of the reference model is shown in Figure 7.4-1.

[1] Bending modes are sorted by frequency after selecting dominant modes for the pitch axis. Additional modes are supported in the model but were truncated to six based on frequency, due to limitations in the F/A-18 surface actuator rates. The maximum supported bending frequency is approximately 3.4 Hz.

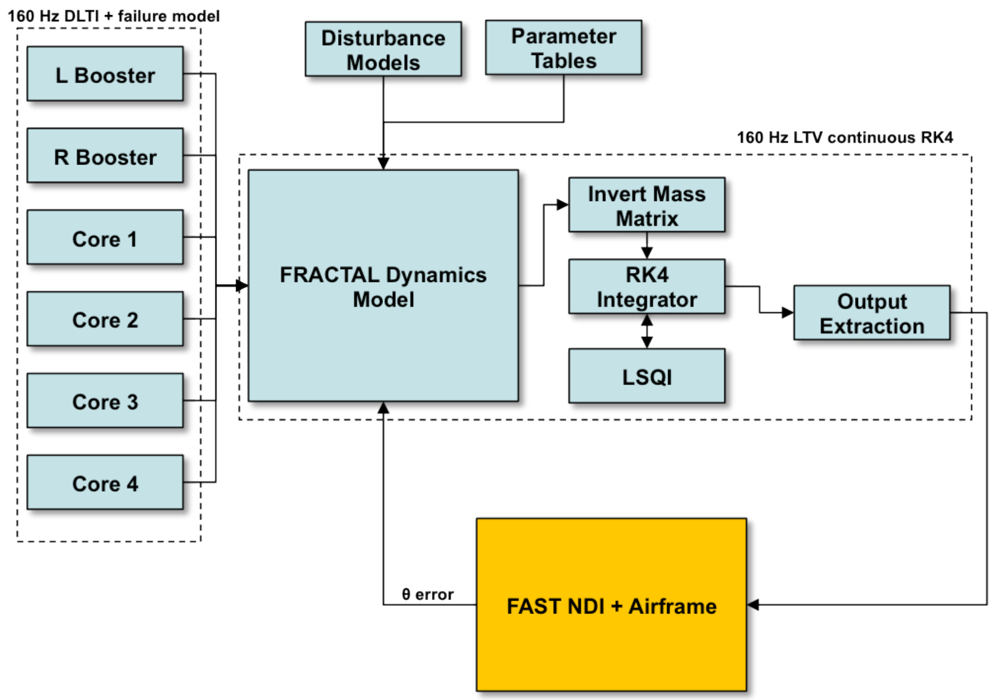

Figure 7.4-1. LVAC Launch Vehicle Reference Model Architecture

Because the LVAC dynamic simulation relied on a single rate reference (e.g., a single inertial measurement unit (IMU)) and the airframe rigid body dynamics were used to simulate the launch vehicle elastic response, direct simulation of multiple-sensor blending was not feasible. However, SLS employs a composite blended sensor output from multiple rate sources, including the forward-mounted redundant inertial navigation unit and the intertank and core aft skirt rate gyro assemblies (RGAs). To support accurate modeling of the sensor blending effects, the simulated elastic rate measurements were combined inside the model prior to generating the reference angular rate output for the FAST inversion controller.

Based on time-and-frequency domain analysis of the aircraft nonlinear dynamic inversion function, it was determined that the low-pass and delay characteristics of the airframe tracking dynamics were similar to those of the true SLS sensor dynamics and transport delay. Since SLS sensor nonlinearities are well characterized and have negligible effect on the boost-phase attitude dynamics, the aircraft sensors (having performance less than that of a launch-vehicle grade navigation instrument) could conservatively capture the dominant effects. Therefore, the SLS sensor models were removed, and the airframe served as an effective surrogate for the SLS sensor and avionics chain.

Internal integration of the continuous-time core vehicle dynamics was performed at the FAST frame rate of 160 hertz (Hz) using a custom Runge-Kutta fourth-order integration routine with support for the LSQI transition logic. The linear portion of the actuator dynamics, where parameters are constant over the flight regime being studied, was explicitly discretized.

Environmental effects and failure injection was implemented in support of LVAC test scenarios. In addition to direct modification of plant parameters (e.g., slosh damping), these features include random (band-limited) turbulence and prescribed wind gust inputs, engine out, actuator hardover and fail-in-place events, and prescribed torque disturbances.

Band-limited turbulence was implemented in terms of a trajectory-relative velocity profile and was generated using a filtered zero-mean Gaussian random profile having a 1– σ[2] α perturbation of 3 degrees with a bandwidth of 0.2 Hz. This profile provided vehicle dynamic excitation, especially sloshing and bending modes, commensurate with the launch vehicle flight environment in the case that the true (flight-day) natural environment was unusually quiescent.

For certain TCs, a wind shear was superimposed on the baseline turbulence profile. This shear profile was derived from a 3-σ Global Reference Atmosphere Model (GRAM) Monte Carlo run used for loads case verification during the CxP Ares I-X vehicle development. This shear was particularly stressing as it accumulates significant bias during the early portion of flight and undergoes a large change in magnitude in the region of maximum q. An example shear profile, including the baseline turbulence profile, is shown in Figure 7.4-2. Note that the profile sign was reversed in shear cases so as to induce a pitch-up disturbance to the F/A-18 airframe near the end of the trajectory. This prevented excessive nose-down attitude of the aircraft just prior to experiment termination.

[2] Internal to the reference dynamics, the angle of attack is computed using a small-angle approximation as a function of the trajectory normal velocity and the simulated (launch vehicle) Earth-relative velocity *V(t)* [ref. 11]. The variance of the velocity profile is scaled by the Earth-relative velocity such that the variance of the resultant angle of attack perturbation is constant (see Figure 7.4-2).

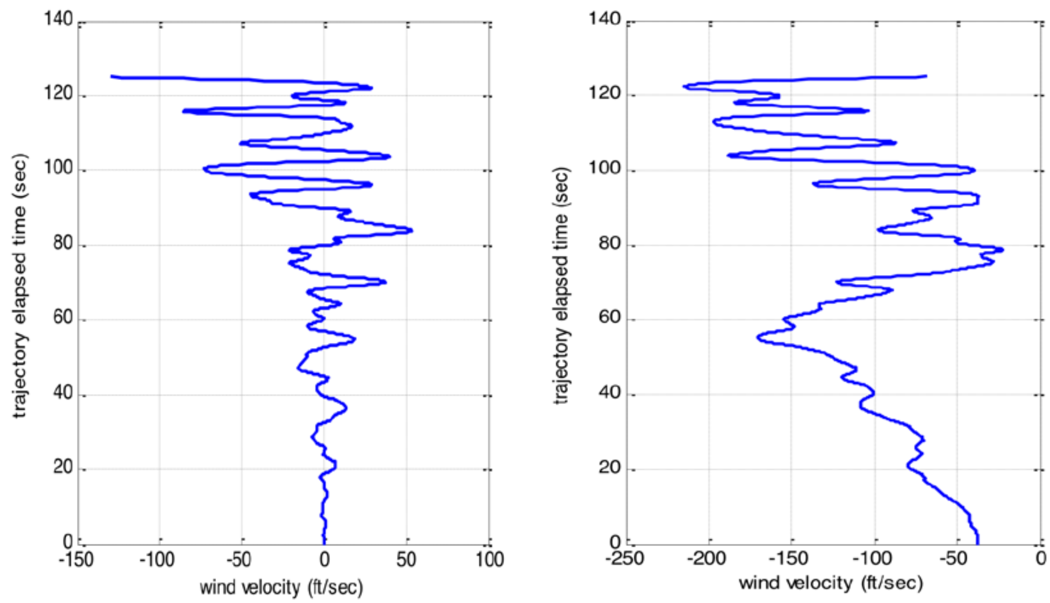

Figure 7.4-2. Reference Model Wind Profiles: Baseline (left) and Shear (right)

To support test operations, outputs of the reference model were used to compute certain termination conditions that were implemented for FAST automated disengage during each trajectory. These conditions indicated the occurrence of a failure mode that was unrecoverable and called for experiment termination. The primary termination conditions indicate a simulated structural load exceedance based on excessive bending strain energy or the product of rigid-body q-α. For the purposes of the LVAC experiment, structural failure was assumed to occur if the simulated vehicle tip deflection exceeded 5 ft or the rigid-body load indicator exceeded 8,500 degree-lbf/ft^2.

The general approach to the derivation of the FRACTAL dynamics for this model was extensively documented in references 15 and 16.

8.0 Flight Control Implementation and Test Scenarios

This section provides an overview of the SLS FCS and its implementation for the flight campaigns. The SLS scenarios that were developed and flown are described herein.

8.1 SLS FCS Overview

The SLS FCS (Figure 8.1-1) is based upon a PID algorithm supplemented by disturbance compensation elements for translation and rotation. The primary mechanism is feedback control of the vehicle attitude dynamics via sensing of attitude errors and vehicle body rates, while simultaneously rejecting parasitic elastic and propellant sloshing dynamic response. In order to effect a load relief and anti-drift function, small adjustments to vehicle attitude are used to control the vehicle translational state with respect to a trajectory-referenced equilibrium.

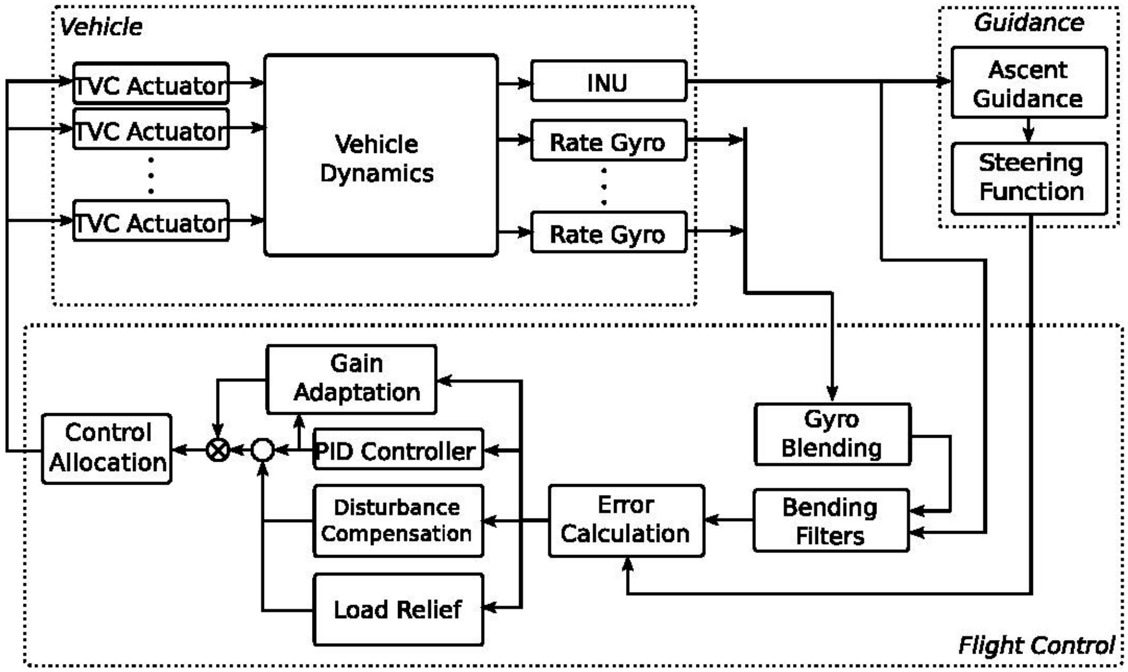

Figure 8.1-1. SLS FCS Overview

Vehicle commands are issued in terms of angular acceleration at a frame rate of 50 Hz (80 Hz in LVAC implementation with appropriate scaling of filter coefficients). The PID controller is preceded by optimized linear bending filters, which provide appropriate phase shaping and gain attenuation such that vehicle flexibility and fuel sloshing dynamics remain adequately attenuated. Filters are implemented in a series fourth-order transfer function mechanization to avoid numerical difficulties encountered with high-order filters (e.g., coefficient truncation and state quantization).

Angular and translational DCAs borrow from the form of the in-flight load-relief/anti-drift algorithms used in the Ares I and Ares I-X autopilots. The DCA elements operate on the principle of constructing estimates of unmeasured dynamical variables (e.g., angular acceleration). These estimates are used to deduce the magnitude of external disturbances, which are compensated with an appropriate lateral or angular acceleration command. Since the disturbance compensation algorithms rely on vehicle lateral acceleration measurements that cannot be reproduced by the FAST platform, the DCA algorithms were not exercised in flight test.

The SLS vehicle relies on pitch/yaw rate data from multiple rate sensors, including two RGAs and the primary IMU located in the forward instrument ring. The three rate measurements are blended using scheduled optimal weights to maximize structural mode attenuation prior to filtering.

Since SLS's multiple-engine configuration yields redundant control authority in three axes, a gain-scheduled linear control allocation scheme is used to optimally allocate commands to the engine actuators to achieve the commanded angular acceleration, while minimizing a weighted norm of the control deflection. Weight computations are performed on-line in the flight software using tabulated *a priori* data detailing the engine locations, vehicle mass properties, and thrust profiles. Online computation allows the algorithm to reconfigure and accommodate a loss of engine thrust, guidance throttling, and the end of the SRB burn with a negligible change in the total loop gain.

Flight certification of the SLS FCS is expected to follow from a classical procedure involving trajectory-relative linearization of the vehicle dynamics and autopilot open loop (annotated in Figure 8.1-1) at discrete operating points supplemented by nonlinear time-domain Monte Carlo simulation and statistical analysis. The Nyquist criterion is applied to the open-loop frequency response, and the linear, time-invariant stability margins are assessed. In addition, the SLS Program has employed a scalar technical performance metric (TPM) based on the Nichols disc margin, analogous to the "point of closest approach" technique used in the Evolved Expendable Launch Vehicle community. The disc margin is calculated in the Nichols plane by computing the scale factor of the largest disc that can be inscribed in the interior of the frequency response near the midpoint of the low-frequency (aerodynamic) and high-frequency (rigid-body) crossings of –180 degrees of phase. The disc scale factor is compared with that of a reference disc that has dimensions based on industry-standard values of gain and phase margin. The ratio between the actual disc and reference disc is used to generate a scalar metric of flight control design margin. Since the disc centroid is allowed to vary independently of the forward loop gain, the analysis process allows the program to allocate classical stability margins to the AAC algorithm without affecting the value of the TPM.

A comprehensive overview of the SLS FCS design can be found in reference 17.

8.2 Flight Software Prototype Implementation

To integrate the SLS FCS with the SLS reference model and F/A-18 NDI controller such that the algorithms could be autocoded onto the ARTS software platform, a Simulink® S-function of the SLS FCS was developed and interfaced to the Simulink® SLS reference model. The S-function passes and receives signals to and from the C/C++ SLS flight software prototype, the same code executed in the SLS GN&C development simulations and in the SIL. The FCS design that was employed, including the digital filter parameters and gains optimized for SLS, matches those used for DAC-2, although the AAC component was updated from the DAC-2 to the DAC-3 implementation as described by Wall *et al.* [ref. 3]. Originally, the entire experiment was designed using the DAC-2 SLS models and FCS. However, flight delays afforded the team the opportunity to integrate AAC algorithm updates that were incorporated into the DAC-3 version of the FCS. The remainder of the FCS and models were based on the DAC-2 versions.

There were several changes made to the flight software prototype to facilitate implementation of the flight experiment. As multiple flight tests were to be flown for a single executable version of the flight software and specific tests contained flight control parameter modifications, adjustments to the original initialization and parameter definition logic were made. In the SLS flight software implementation, a single parameter initialization function suffices for a single flight. For the LVAC experiment, logic was employed to allow for selection amongst a precompiled set of initialization functions, each having unique parameter sets. Additional modifications to the initialization functions were made to ensure the internal variables containing history (e.g., integrators, filter states) were reset between executions of subsequent TCs. Since the FCS architecture has the same form across all axes, for simplicity the control experiment for LVAC was implemented on the pitch-axis only. In the operational SLS vehicle, the control allocation framework accounts for the SRB TVC system being rotated 45 degrees about the booster roll axis (TVC actuation is split between the pitch and yaw axes). Since this is a pitch-only experiment, the control allocator within the FCS, as well as the SLS reference model, assumed the TVC system to be in-plane with the pitch axis. The controller was modified to schedule gains and parameters with respect to SLS trajectory time rather than other navigated independent variables used in the production system. The SLS FCS includes attitude rate sensor blending, but the effects of sensor blending were moved into the dynamics model since the aircraft uses a single sensor for attitude and rate. In contrast, the SLS requires a blend of multiple sensor measurements to achieve attenuation of structural modes. The autopilot's discrete filters were reoptimized for the same phase and attenuation constraints as the original 50-Hz filters, but with a modified rate at 80 Hz to accommodate the update rate of the F/A-18 pitch axis control system. An example rate error filter comparison for the max-q portion of the SLS ascent flight is shown in Figure 8.2-1. The filter response only needed to match in the basic shape and attenuation to provide ample stability in the nominal cases and allow for intentional destabilization of flex modes in off-nominal cases, while providing traceability to the SLS DAC-2 configuration design requirements. The only part of the SLS autopilot architecture disabled for the LVAC experiment was the DCA since the spacecraft translational dynamics could not be replicated by the aircraft.

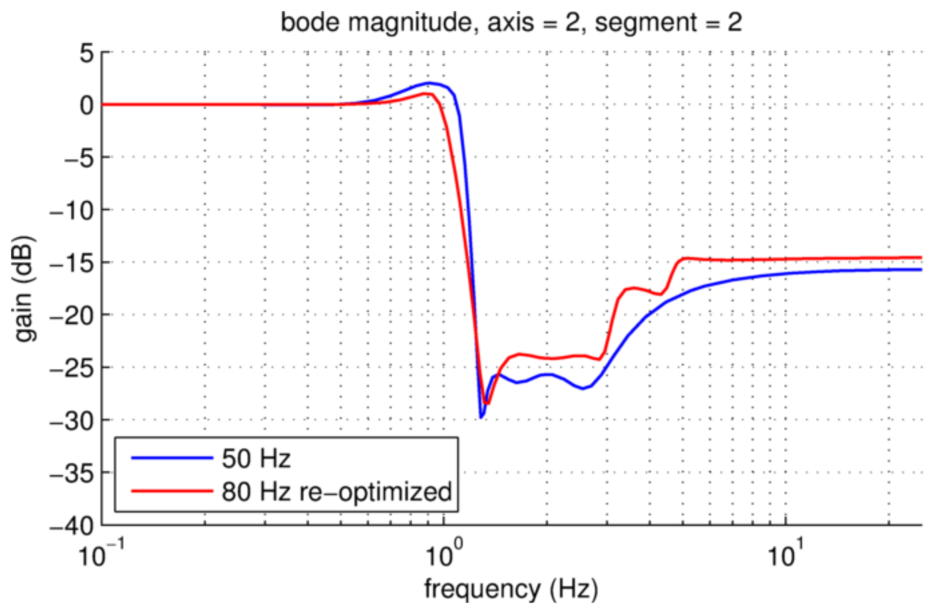

Figure 8.2-1. Comparison of Pitch Rate Filter after Reoptimization at Target Update Rate

8.3 Description of SLS Scenarios Implemented During Flight

Several scenarios were designed based on the SLS DAC-3 models. Vehicle, environmental, and/or control parameters were modified to simulate TCs based on extreme, but physically realizable scenarios that map into the flight test objectives. These TCs are summarized in Table 8.3-1, and complete descriptions are provided in Appendix B.

Table 8.3-1. Full Set of TCs Generated for Research Flights

TC	DESCRIPTION	OBJ	AAC	FT 1	FT 2	FT 3	FT 4	FT 5
0	Nominal plant, environment, and controller	1	OFF	A	A		M(2)	M(2)
			ON	A(3)	A(2)		M(2)	M(2)
1	Heavy/slow vehicle	1	OFF			A		
			ON			A		
2	Light/fast vehicle	1	OFF			A		
			ON			A		
3	Wind shear event	2	OFF		A			
			ON		A			
4	TVC bias	2	OFF		A(2)			
			ON		A			
5	Hardover failure of two core engines (offset in time)	2	OFF		A		M	M
			ON		A		M	M

6	HEAVY/SLOW, WIND SHEAR, SRB TAILOFF THRUST IMBALANCE	2	OFF			A		
			ON			A		
7	Wind shear event and double hardover failure	2	OFF		A		M	M
			ON		A		M(2)	M
8	Case Breach	2						
9	Light/fast with slosh instability	3	OFF		A	A		
			ON		A	A		
10	Structural instability	3	OFF		A(2)	A		
			ON		A	A		
11	Thread-the-needle I	2&3						
12	Thread-the-needle II	2&3						
13	Low-gain controller with wind shear event	2						
14	Low-gain controller, wind shear, 2 hardover failures	2	OFF		A			
			ON		A			
15	High-gain controller, slosh instability	3	OFF		A	A		MA(2)
			ON		A	A		MA
16	High-gain controller, unstable flex	3	OFF		A	A	MA(2)	
			ON		A(2)	A	MA	
17	High-gain controller, rigid body instability	3	OFF		A	A	MA(2)	MA(2)
			ON		A	A(2)	MA(2)	MA(2)
18	High-gain controller, structural and slosh instabilities	3						
19	Identification of F/A-18 structural mode	3	OFF	S/L(3)				
20	F/A-18 structural mode amplification with inertial navigation system (INS)	3	OFF				S/L	S/L(2)
			ON				S/L	S/L
21	Ground test mode	This mode used for preflight checks						
22	F/A-18 structural mode amplification with embedded global positioning system (GPS) INS (EGI)	3	OFF				S/L	S/L(4)
			ON				S/L	S/L(2)

"A" – Experiment conducted in *autopilot* mode; "M" – *manual* mode (pilot steering commands); "S/L" – straight and level flight; number in parentheses indicates number of times TC was flown if greater than 1; gray rows represent TCs that were designed but did not fly.

Each of these TCs was simulated at MSFC with a reduced-order time-varying F/A-18 model in the loop with the AAC both off and on. Each case was subsequently tested with the AAC off and on in the F/A-18 HILS at AFRC. Finally, a subset of the TCs was flown on the FAST aircraft.

9.0 Summary of Research Flights and Results

Two series of flights have been conducted using the SLS autopilot prototype software on the FAST platform. The first series consisted of three flights completed on November 14–15, 2013. During these three flights, an F/A-18 structural mode identification test was completed while in level flight, as well as 46 SLS-like trajectories in autopilot mode, which were designed to match predefined SLS scenarios. The structure of the initial test series was such that at the conclusion of the first series the principal AAC design objectives (1 through 3) had been successfully demonstrated multiple times.

During the second flight campaign completed on December 11–12, 2013, the emphasis shifted to amplification and recovery of a physical airframe mode using identification data from the first campaign, exploring interactions between manual steering and AAC, and repeating SLS scenarios that had exhibited in-flight variability. Approximately 13 straight and level tests were completed to demonstrate the ability of the AAC to mitigate an intentionally destabilized airframe structural mode, and 45 SLS-like trajectories were flown across three sorties.

A brief description of the SLS scenarios flown is provided in Tables 9.1-1, 9.2-1, and 9.3-1. TCs completed to explore interactions between manual steering and the AAC are indicated in the aforementioned tables. A more complete summary of each sortie is tabulated in Appendix A.

9.1 Flight Test Results for Near-nominal SLS Scenarios (Objective 1)

The first flight objective was intended to show negligible adaptation in an environment that is commensurate with the nominal controller design envelope. Three TCs were flown that map into this objective, as shown in Table 9.1-1. Each of the TCs was flown with the AAC on and off for comparison.

Table 9.1-1. Flight-tested Objective 1 Scenarios/TCs

TC	DESCRIPTION	AAC	FT 1	FT 2	FT 3	FT 4	FT 5
0	Nominal plant, environment, and controller	OFF	A	A		M(2)	M(2)
		ON	A(3)	A(2)		M(2)	M(2)
1	Heavy/slow vehicle	OFF			A		
		ON			A		
2	Light/fast vehicle	OFF			A		
		ON			A		
"A" – Experiment conducted in *autopilot* mode; "M" – *manual* mode (pilot steering commands); number in parentheses indicates number of times TC was flown if greater than 1.							

In the absence of adaptation, the total adaptive gain multiplier, shown in Figure 9.1-1, would be unity. The flight test results are consistent with the MSFC simulation and the AFRC HILS and show little adaptation. There is a small but out-of-family decrease in the total loop gain shortly after 60 seconds, which was caused by a pitch transient induced by the pilot de-throttle command near the trajectory crest. The pitch error and left booster angle (illustrating control usage) are shown in Figure 9.1-2, showing excellent matching across simulations and flight with little adaptation. The other test scenarios showed similar results, further demonstrating minimal adaptation inside the normal SLS flight envelope and satisfying objective 1.

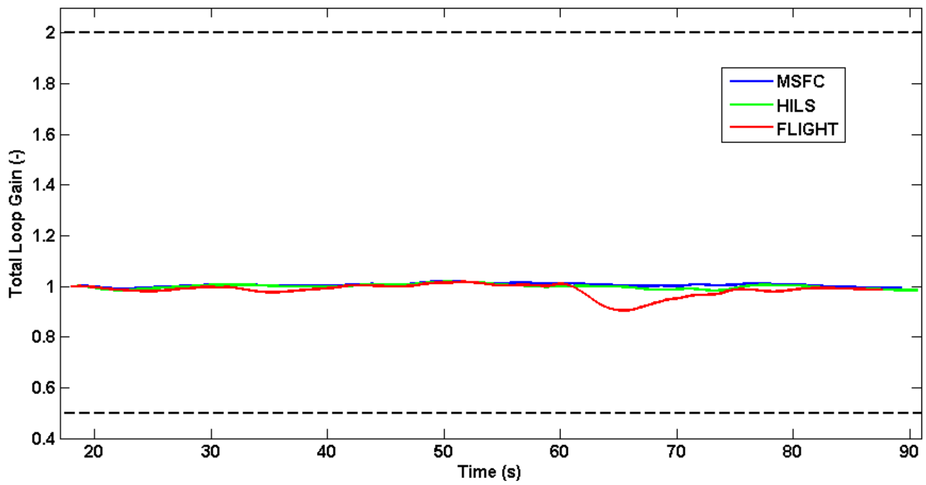

Figure 9.1-1. Adaptation of the Total Loop Gain (nominal SLS scenario)

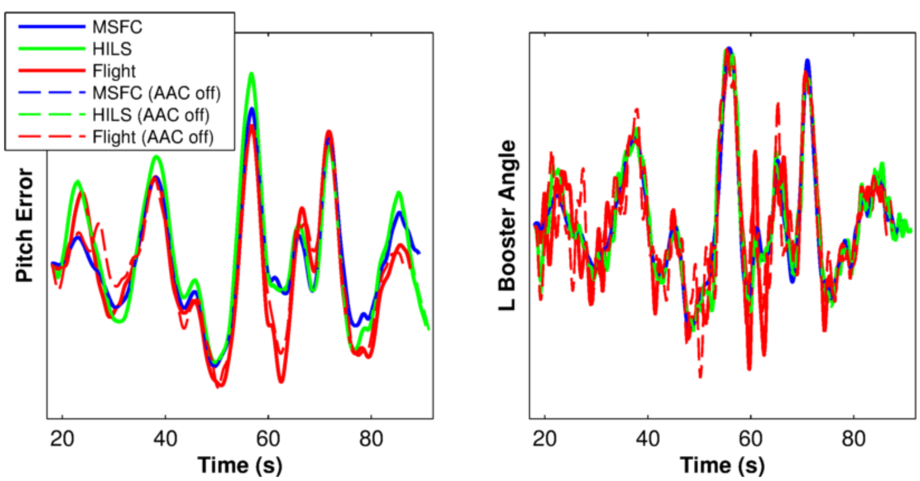

Figure 9.1-2. Results for the Nominal SLS Scenario

9.2 Flight Test Results with Low Performance SLS Scenarios (Objective 2)

The second flight objective was to demonstrate improved performance in an environment where the nominal controller performance is poor. To generate these scenarios based on SLS dynamics, key parameters within the model, controller, and environment were modified to create stressing conditions to challenge the fixed-gain control system. Table 9.2-1 contains a description of the SLS conditions for each objective 2 test scenario. In several cases, slosh dynamics were disabled to isolate the effects of the simulated rigid body or elastic instability.

In the cases involving wind disturbances, the SLS aerodynamic instability was exaggerated to further stress the baseline attitude controller.

Table 9.2-1. Flight-tested Objective 2 Scenarios/TCs

TC	DESCRIPTION	AAC	FT 1	FT 2	FT 3	FT 4	FT 5
3	Wind shear event	OFF		A			
		ON		A			
4	TVC bias	OFF		A(2)			
		ON		A			
5	Hardover failure of two core engines (offset in time)	OFF		A		M	M
		ON		A		M	M
6	Heavy/slow, wind shear, SRB tailoff thrust imbalance	OFF			A		
		ON			A		
7	Wind shear event and double hardover failure	OFF		A		M	M
		ON		A		M(2)	M
14	Low-gain controller, wind shear, two hardover failures	OFF		A			
		ON		A			
"A" – Experiment conducted in *autopilot* mode; "M" – *manual* mode (pilot steering commands); number in parentheses indicates number of times TC was flown if greater than 1.							

All of the objective 2 scenarios exhibited excellent matching between the MSFC simulated results, AFRC HILS predictions, and the flight tests. This matching is exemplified here through the results of TC 7, shown in Figures 9.2-1 and 9.2-2. This SLS-derived scenario features a wind shear event followed by two core engine hardover failures. This scenario would have forced the SLS without the benefit of the AAC to exceed the structural limits shortly after 60 seconds, at which time the TCs are discontinued, as observed in Figure 9.2-2. In the AAC-on scenarios, the on-line gain adjustment improves the response time of the controller to the disturbance, keeping the SLS within the limits of the structural load indicator without requiring excessive control commands (see Figures 9.2-1 and 9.2-2). Thus, the AAC algorithm meets the objective of increasing the total loop gain in response to excessive error in the pitch attitude beyond what would be expected within a normal flight envelope. Other TCs that map to this objective produced similar results, thereby increasing the confidence that the AAC improves the SLS vehicle performance under anomalous conditions.

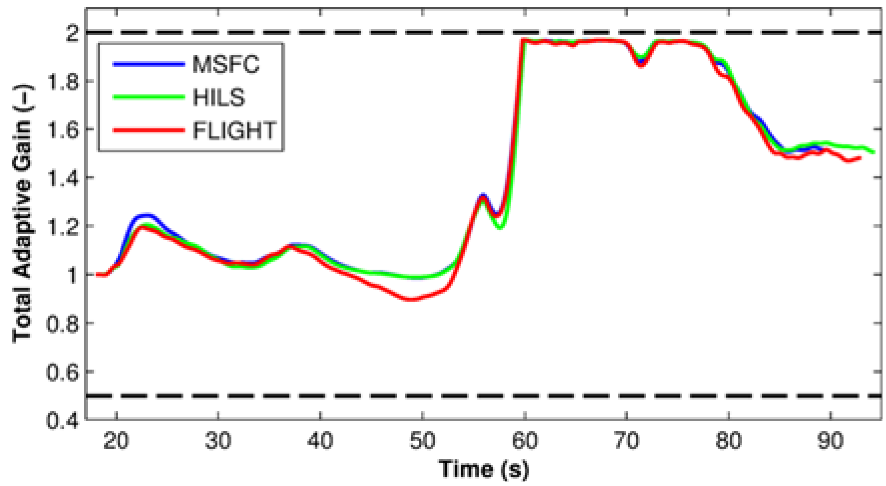

Figure 9.2-1. Adaptation of the Total Loop Gain (low performance scenario)

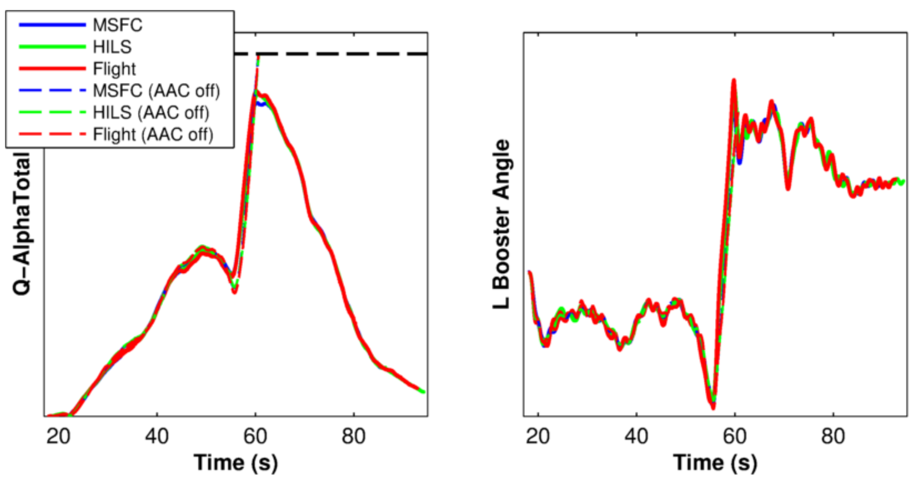

Figure 9.2-2. Low Performance Results

9.3 Flight Test Results with Unstable Parasitic Dynamics (Objective 3)

The third flight objective was to demonstrate the AAC's ability to restrict unstable, mismodeled parasitic dynamics to a small-amplitude, nondestructive limit cycle. The TCs associated with this objective are shown in Table 9.3-1. Matching the high-frequency, unstable SLS parasitic dynamics with the F/A-18 for objective 3 TCs was more challenging than with tracking the SLS dynamics for the objective 1 and 2 scenarios. Contributing to the difficulty in matching the high-frequency SLS dynamics is the bandwidth available to the NDI for generating the necessary frequency content and magnitude. The NDI is sensitive to the aircraft q, which varied throughout the maneuver and from trajectory-to-trajectory depending on the initial conditions of the maneuver. Thus, the resulting pitch attitude and rate amplitude were a function of the initial condition at the time the experiment is engaged. Furthermore, the aircraft inertia properties change significantly as a function of fuel level. To better understand these variations and provide data for the analysis of the NDI performance for high-magnitude, high-frequency modes, each of the scenarios listed was repeated at various initial conditions and aircraft fuel states.

Table 9.3-1. Flight-tested Objective 3 Scenarios/TCs

TC	DESCRIPTION	AAC	FT 1	FT 2	FT 3	FT 4	FT 5
9	Light/fast with slosh instability	OFF		A	A		
		ON		A	A		
10	Structural instability	OFF		A(2)	A		
		ON		A	A		
15	High-gain controller, slosh instability	OFF		A	A		MA(2)
		ON		A	A		MA
16	High-gain controller, unstable flex	OFF		A	A	MA(2)	
		ON		A(2)	A	MA	
17	High-gain controller, rigid body instability	OFF		A	A	MA(2)	MA(2)
		ON		A	A(2)	MA(2)	MA(2)
19	Identification of F/A-18 structural mode	OFF	S/L(3)				
20	F/A-18 structural mode amplification with INS	OFF				S/L	S/L(2)
		ON				S/L	S/L
22	F/A-18 structural mode amplification with EGI	OFF				S/L	S/L(4)
		ON				S/L	S/L(2)

"A" – Experiment conducted in *autopilot* mode; "M" – *manual* mode (pilot steering commands); "S/L" – straight and level flight; number in parentheses indicates number of times TC was flown if greater than 1.

Results are shown for TC 16, where the FCS gains were increased and the gain on one of the elastic modes was increased to simulate closed-loop instability. The flex dynamics were applied to the aircraft via the ailerons, and alternate effectors (i.e., primarily stabilators) were used for implementation of the FCS commands. The flaps were mixed in with the stabilators, but to a small extent, and are primarily scheduled with α for aircraft trim. Figure 9.3-1 shows the total loop gain at its initial value of 1, then decreasing rapidly at approximately 35 seconds when the SLS model disturbance was applied to excite the closed-loop instability of the elastic mode. As the instability grows, the frequency content enters into the SLS control command and the AAC responds by decreasing the loop gain to its limit of 0.5. The vehicle deflection is shown in Figure 9.3-2, with the SRB TVC command. The amplitude of the elastic deflection was higher during flight than observed in either simulation. This was due to the reduced performance of the NDI caused by the aileron-generated moments at the SLS mode frequency being higher than predicted by the simulation and assumed by the NDI aerodynamic coefficient tables. The resulting larger amplitude instability could not be eliminated with the total loop gain at its minimum value. The simulated LOV was delayed for approximately 10 seconds, which was considered a significant accomplishment. A similar trend was seen in TC 10, which used the aircraft's ailerons to provide motion corresponding to simulated flex instability. TCs 9, 15, and 17, which used alternate control surfaces, were able to demonstrate stabilization (i.e., reduction to a low-amplitude limit cycle) through the use of AAC.

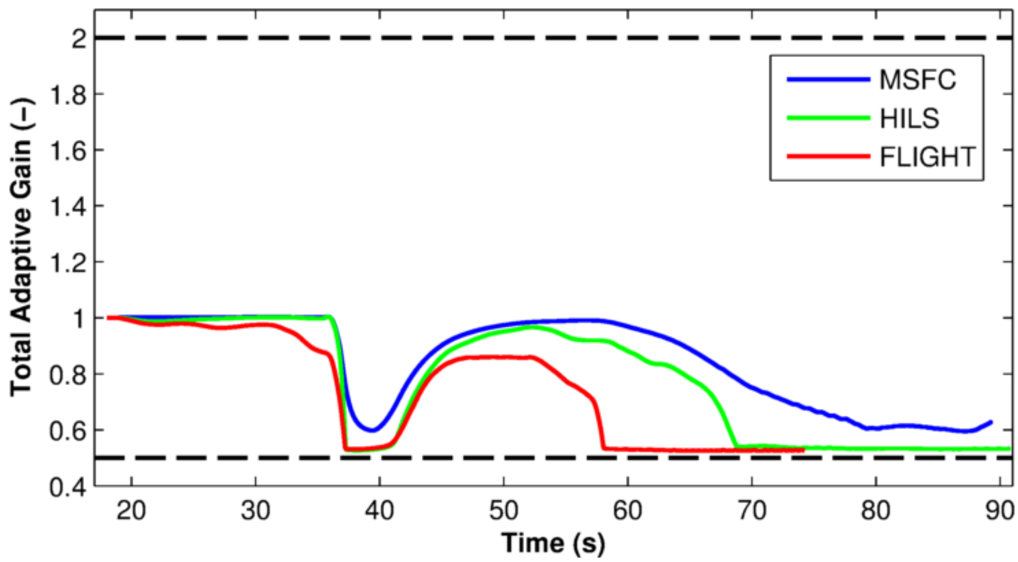

Figure 9.3-1. Adaptation of the Total Loop Gain (fictitiously unstable, flexible body dynamics)

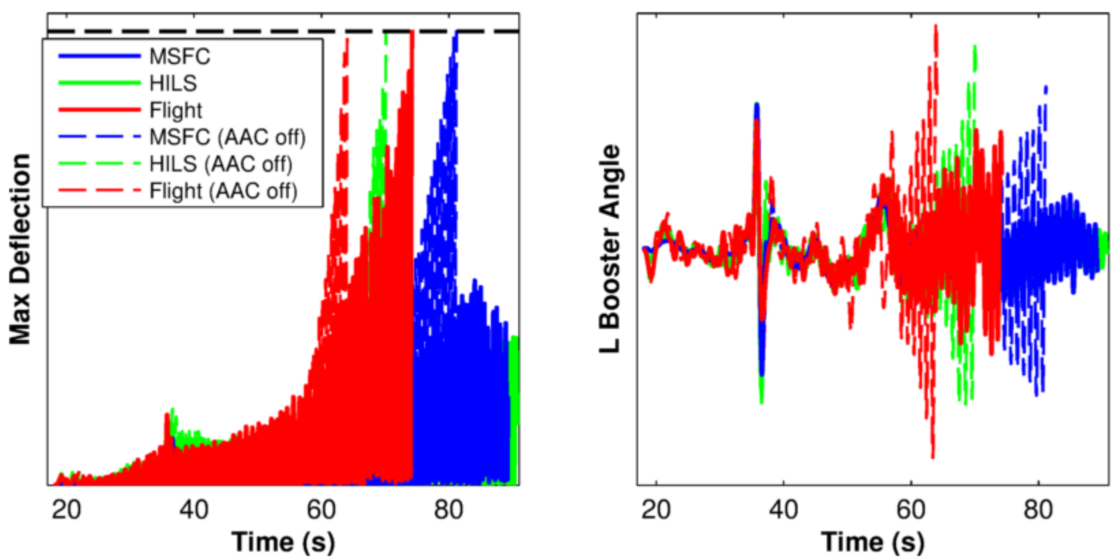

Figure 9.3-2. Results for the Fictitiously Unstable Flexible Body Dynamics

9.4 Airframe Structural Mode Identification and Amplification Test (Objective 3)

The objective 3 TCs for the majority of the research flights demonstrated stabilization of unstable SLS structural modes, slosh, or rigid body dynamics as implemented in the SLS reference model within the aircraft's software. These instabilities were driven by control surfaces and measured through the resultant aircraft rigid body response. Additional tests were conducted to further demonstrate the ability of the AAC algorithm to attenuate unfavorable interaction between the control system and the physical F-A/18 structural dynamic response. During the first research flight, tests were conducted to identify the primary aircraft pitch structural mode of the airframe from the symmetric stabilator command to the pitch rate response at each of the two sensor packages. During the second series of flights, TCs were flown so that, using a high-gain filter, intentionally destabilized the closed-loop response with the F/A-18 airframe mode and demonstrated the ability of the adaptive element to suppress the divergent response. For both sets of tests, the baseline F/A-18 filters on the pitch rate feedback to the SLS controller were set to unity, while the filters in the FAST NDI feedback paths were maintained. In addition, the SLS controller attitude error and rate error filters were set to unity, and the SLS reference model slosh dynamics, flex dynamics, and actuator limits were all disabled. These adjustments yielded a simple system in which the SLS FCS with adaptive element interacts with the FAST NDI and the basic F/A-18 airframe.

To identify the structural response, a 60-second phase-optimized multiple-sinusoid PTI signal [ref. 18] was added to the SLS angular acceleration control command with a frequency range around the expected resonance. The magnitude of the resultant PTI waveform was configurable in flight with subsequent presses of the nosewheel-steering button. The highest magnitude of the five available values corresponded to the point at which the stabilators were predicted to reach actuator rate saturation based on observations during the HILS V&V simulation. The in-flight adjustability of the test input magnitude allowed for a buildup approach to ensure the safety of the airframe and pilot in the case of unexpectedly high response magnitudes or other unpredicted behaviors. For each of the modal identification test segments, the pilot selected the desired PTI magnitude as indicated by the control room, engaged the experiment during straight and level flight, and thereafter maintained speed and altitude (approximately constant q) with stick motions. In total, three 60-second segments were flown, each with increasing magnitude. Figure 9.4-1 shows the frequency response as reconstructed from the flight data using the second largest magnitude PTI.

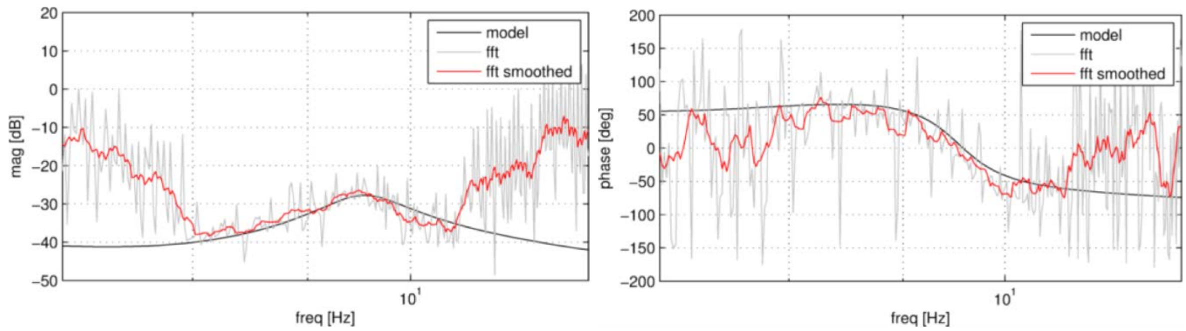

Figure 9.4-1. F/A-18 Airframe Mode Reconstructed Frequency Response

After obtaining the reconstructed flight results, a simple second-order linear model (i.e., parameterized by frequency, damping, gain, and delay) of the structural mode was superimposed with the rigid body dynamics model and fitted to the flight data. The resulting model (shown by lines labeled "model" in Figure 9.4-1) was used to design an eighth-order bandpass filter [ref. 19] to place in the control path, so the structural mode was amplified to instability, but within the capability of the AAC to mitigate the divergent response. The bandpass filter, shown in Figure 9.4-2, was placed on the SLS FCS output to avoid amplification of sensor noise into the AAC spectral damper and to effect direct frequency shaping of the total system response. To allow tuning of the magnitude and phase in-flight, four gain options and five frame delay options were applied in series with the amplification filter.

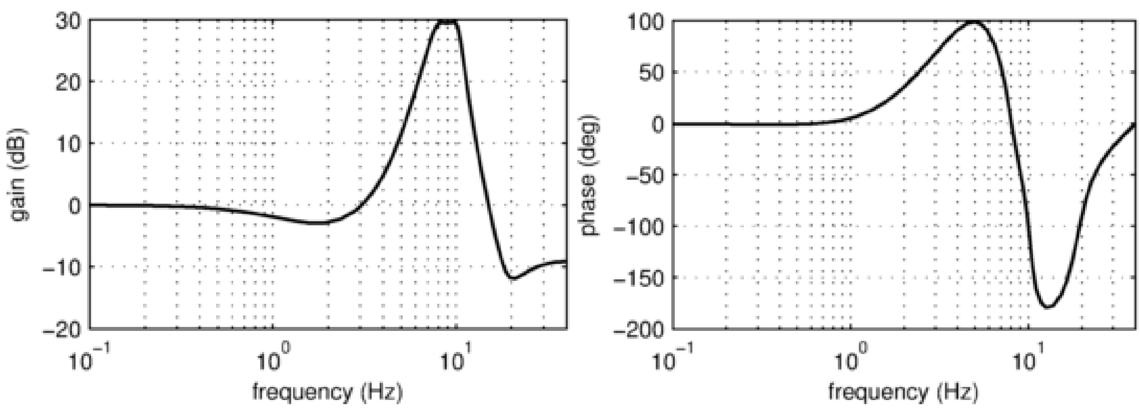

Figure 9.4-2. Airframe Resonance Amplification Filter

For the modal amplification TCs, the bandpass filter was applied, and delay conditions were configured in-flight to achieve a structural instability within the AAC capability to recovery. During the first test segments of the second phase of research flights, the pilot engaged the amplification experiment at the straight and level flight conditions flown during the identification tests.

Figure 9.4-3 shows the results from the amplification tests flown with the AAC disabled and enabled. In each case, a short, attenuated burst of the original PTI signal is scheduled at the

5-second mark to excite the structural resonance. For the case in which the AAC is disabled, the symmetric stabilator response (i.e., black line, left plot) diverges until reaching a limit cycle constrained by its maximum actuator rate capability. When the AAC is enabled, the total loop gain is decreased (i.e., red line, right plot), yielding a reduced control response with significantly increased margin from its rate limits. This TC demonstrated the ability of the AAC algorithm to recover from an unstable physical structural resonance. Additional details regarding the airframe structural mode identification and amplification test are documented in Appendix C.

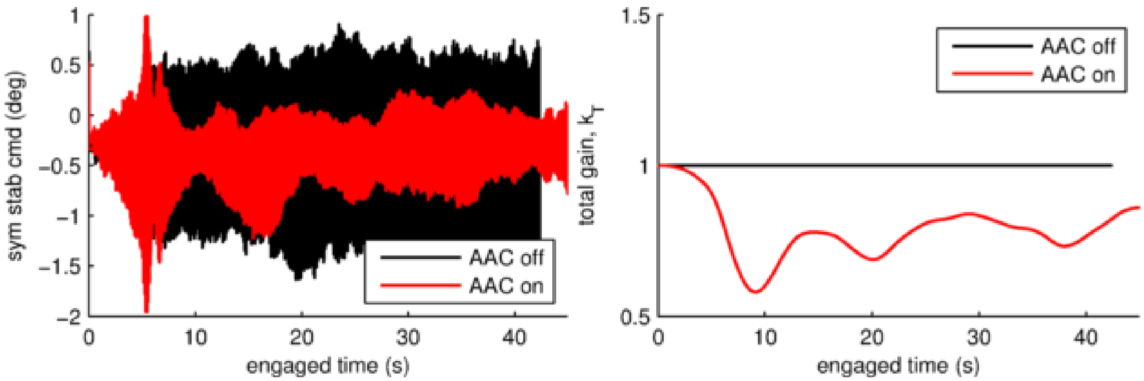

Figure 9.4-3. Airframe Structural Mode Recovery TC Results

9.5 Evaluation of Manual Steering Mode (Objective 4)

Manual steering is a human-in-the-loop attitude control mode under consideration for the SLS. Manual steering allows the crew to have direct, onboard control of the SLS trajectory through the FCS after SRB separation. Manual control introduces an additional dimension of uncertainty into the robustness analysis of aerospace vehicles, given the ability of the pilot to adjust the closed-loop gain of his or her dynamic response [ref. 20]. This variability is especially relevant when coupled to adaptive FCSs (e.g., AAC) that adjust the system gain. When the pilot and the adaptive system make gain adjustments based on the same feedback parameters (e.g., tracking error), the potential exists for adverse interactions [refs. 21–23].

Experimental characterization of this interaction with critical analysis from pilot evaluations may assist in determining whether the AAC should remain active if manual steering is engaged in the event that the SLS Program decides to employ a manual steering mode for the operational vehicle. For this reason, the fourth objective to explore interactions between manual steering and the AAC was added to the LVAC experiment. No official SLS manual steering design existed prior to the flight experiment, so the test team implemented a prototype design, shown in Figure 9.5-1, based on assumed system requirements. It should be noted that the flight test results will inform the official design, and that any flaws discovered in the prototype may not be present in the final manual steering mode architecture.

During the research flights, the ILS glideslope deviation needle on the attitude reference indicator (ARI) displayed pitch attitude error to the pilot. The ARI position at the top of the instrument panel, near the heads-up display (HUD), allowed the pilot to maintain external situational awareness. Pitch rate control inputs were made through control stick longitudinal deflection. The pilot lateral stick and rudder pedals were disabled with the SLS control laws engaged. A separate autopilot maintained lateral-directional control.

As shown in Figure 9.5-1, the pilot control input was a rate command proportional to pitch stick deflection. This rate command was integrated to allow both rate and attitude errors to be computed and used as inputs to the control laws. The trajectory cue displayed to the pilot was a fixed –0.75-degree/second nose-down command.

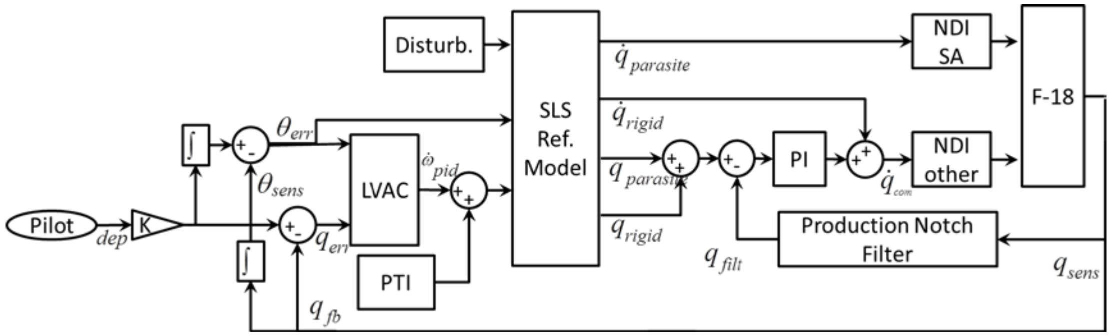

Figure 9.5-1. Manual Steering Mode Implementation

The LVAC experiment gathered data for 25 test trajectories flown under manual steering mode, 13 with Pilot A on flight 143, and 12 with Pilot B on flight 144. The 25 test trajectories consisted of six different TCs covering the three main test objectives. TCs represent extreme events outside the SLS design envelope. Table 9.5-1 lists the manual steering mode test matrix.

In most instances, both pilots evaluated a given TC to account for differences in technique and rating methodology. Back-to-back evaluations with and without adaptation helped reduce uncertainties due to atmospheric and aircraft mass property variations. The “nominal plant and environment” TC was evaluated at the beginning and at the end of each flight to establish a trend for pilot adaptation to the task.

Table 9.5-1. Manual Steering Mode Test Matrix

Objective	TC	Scenario Description	Card	AAC On	Pilot A (No. of Test Points)	Pilot B (No. of Test Points)
1	0	Nominal plant and environment	5	YES	2	2
			6	NO	2	2
2	5	Two-spaced hardover failures	7	NO	1	1
			8	YES	1	1
	7	Wind shear, two hardover failures	11	NO	1	1
			12	YES	2	1
3	15	High gain plus slosh excitation	25	NO	--	1
			26	YES	--	1
	16	High gain with unstable flex	19	NO	1	--
			20	YES	1	--
	17	High gain plus rigid body instability	29	NO	1	1
			30	YES	1	1

Test pilots rated each configuration using the aircraft pilot-in-the-loop oscillation (PIO) rating scale [ref. 24]. Ratings were given immediately following the completion of each test point. The aircraft communication system transmitted comments made by the pilot during the test point to the ground control room for situational awareness. This audio stream was recorded with HUD video for post-flight analysis, from which the pilot comments were transcribed and documented in Appendix E.

A more complete discussion and analysis of the manual steering mode test results can be found in Appendix D, with a description of the metrics used to evaluate the manual steering mode and its interaction with the AAC. In order to explore the interactions between manual steering and AAC, scenarios from each of the first three flight objectives were repeated with manual steering engaged. A short discussion of the observations for each of the three objectives is provided in the following sections.

9.5.1 Objective 1 TC with Manual Steering

An analysis of the manual steering mode for TC 0, “Nominal plant and environment” indicate that the pilot and the adaptive controller interact in such a way as to reduce the adaptive gain below its ideal value of 1. Even moderately aggressive pilot commands are of high enough frequency to be detected as parasitic dynamics by the spectral damper and cause the adaptive gain to be lowered. The reduction in forward-loop gain lowers the vehicle responsiveness to the pilot’s commands, which may invite more aggressive manual inputs. These inputs further reduce the adaptive gain, and the result is a tendency by the pilot to over-command the system with large, aggressive inputs, causing the adaptive gain to decrease to its lower limit. Although the test pilots showed an ability to alter their piloting technique to reduce unwanted interactions, the system showed higher than desired pilot workload and a strong tendency for pilot-involved oscillations in the presence of large tracking errors or external disturbances.

These results underscore a key assumption in the design of the AAC: that the presence of parasitic dynamics in the bandwidth of the spectral damper is indicative of a loop gain that is too high and that the correct response is to reduce the adaptive gain. In some cases, the use of manual steering mode violates this assumption. Although none have been identified for the SLS, it is conceivable that other sources of internal or external unmodeled dynamics, for example, external guidance or steering algorithms, may cause the AAC to adjust its gain in a way that further excites those dynamics or fails to attenuate them.

9.5.2 Objective 2 TCs with Manual Steering

Two TCs were flown to evaluate manual steering mode under objective 2:

- TC 5: Two spaced hard-over failures
- TC 7: Wind shear and two simultaneous hard-over failures

For TC 5, the tracking performance was equivalent between the automatically and manually flown points when the AAC was off. Activation of the adaptive controller improved performance of the autopilot but resulted in larger tracking error under manual steering control.

In TC 7, the ideal response of the adaptive gain is to remain near 1 until the failure occurs and then increase toward the maximum value of 2. On the first manual steering attempt by Pilot A, the adaptive gain oscillated between the minimum and maximum value, making the vehicle response unpredictable to the pilot. The high-workload pilot commands are detected by the spectral damper and tend to drive the adaptive gain toward its minimum.

The use of manual steering mode in conjunction with the AAC for off-nominal scenarios in which control effectiveness is overpredicted (e.g., TCs 5 and 7) lowered tracking performance as compared with the autopilot.

- With the AAC off, manual steering mode had about the same error as the autopilot
- With the AAC on, manual steering mode had significantly more tracking error than the autopilot

9.5.3 Objective 3 TCs with Manual Steering

Three objective 3 TCs with manual steering mode were evaluated:

- TC 15: High gain controller with slosh excitation (Pilot B)
- TC 16: High gain controller with unstable flex (Pilot A)

- TC 17: High gain controller with rigid body instability (Pilots A and B)

In TC 15, the autopilot stabilized the slosh mode with and without the adaptive controller. However, the control commands of Pilot B, without adaptation, excited the slosh mode into an instability that caused the system to violate its internal q-α limit near the 76-second point of the trajectory. With the AAC on, Pilot B was able to complete the trajectory with only marginally worse tracking performance than the automatic system.

In TC 16, the unstable flex mode violated the SLS vehicle deflection limit for all attempts. The adaptive controller delayed the limit violation. There was little difference between the autopilot and manual steering with the AAC enabled. Without adaptive control, the pilot extended the length of the trajectory by approximately 9 seconds as compared with the autopilot without AAC.

TC 17 was the only objective 3 manual steering mode evaluation performed by both pilots. Without adaptive control, the unstable rigid body dynamics caused simulated LOV due to q-α violations for the autopilot and the manually flown trajectories. With adaptive control, command inputs by the pilots caused the adaptive gain to reach and maintain its minimum value for the duration of the trajectory, whereas under autopilot control the adaptive gain periodically returned toward the nominal unity value before being driven lower again.

Manual steering mode, due to the higher frequency content of pilot inputs, resulted in lower adaptive gains for cases in which the design gain was too high, but did not result in improved tracking performance.

- The use of manual steering mode has the effect of lowering the adaptive gain, which is beneficial for cases where the vehicle loop gain is too high.
- Certain types of mismodeled dynamics (e.g., slosh modes and rigid body modes) may contribute to unstable PIOs. The AAC can help reduce, but not eliminate the likelihood of these events.

9.6 Summary of Results

The ability of the SLS FCS to recover from adverse flight conditions using adaptation has been conclusively demonstrated through a series of flight tests. Many of the simulated flight conditions could not be suitably accommodated in the absence of the adaptive algorithm. The AAC functionality was as expected in all scenarios and the flight data matched the SIL and HILS simulation results in the low-performance and near-nominal TCs. For the objective 3 cases exhibiting more deviation from the preflight simulation predictions, the AAC was still shown to recover from or significantly delay the consequences of instability. The number of successful trajectories demonstrated in this flight test, in addition to the simulated trajectories, advances the confidence of the SLS Program toward employing the AAC algorithm.

Although the research flights demonstrated that AAC can aid the vehicle's ability to retain stable flight control and limit flight loads during certain adverse scenarios, manual steering interactions with the AAC as-implemented can increase the probability of an adverse pilot-vehicle interaction. Thus, if a manual steering mode is used in subsequent missions, design changes or fade-out of the adaptive component upon engagement may be needed.

10.0 Findings, Observations, and NESC Recommendations

10.1 Findings

The following findings were identified based on the SLS-based scenarios that were flight tested:

F-1. The SLS AAC was confirmed to have minimal impact on the response of the FCS for nominal or near-nominal scenarios.

F-2. The SLS AAC was able to consistently enhance the robustness of the fixed-gain FCS such that it could compensate for physically realizable launch vehicle scenarios with low-performance or unstable internal dynamics.

F-3. Inputs made by the pilot through manual steering during a nominal or low-performance launch vehicle scenario tend to suppress the AAC gain below the value that provides the best combination of performance and robustness.

F-4. The AAC algorithm can increase the probability of an adverse pilot-vehicle interaction if the SLS manual steering mode is engaged during a nominal or low-performance scenario.

10.2 Observations

The following observations were identified:

O-1. The manual steering mode evaluated does not reflect the SLS manual steering design as this operational mode has not yet been designed.

O-2. The likelihood and severity of adverse interactions between the pilot and the AAC can be reduced through modifications in pilot technique.

O-3. Pilot steering did not enhance vehicle performance or robustness beyond what could be achieved by the SLS FCS (inclusive of the AAC) although under certain failure scenarios the pilot could outperform the fixed-gain control system (without the AAC).

O-4. The F/A-18 FAST aircraft and AFRC engineering and operations personnel are highly qualified to perform research flights that emulate the dynamics of other aircraft, launch, or reentry vehicles in support of GN&C algorithm development and software validation.

10.3 NESC Recommendations

The following NESC recommendations are directed to the SLS Program.

R-1. Continue use of the AAC algorithm as part of the SLS FCS pending its maturation through standard design cycle analyses, stability analysis, and SIL testing. ***(F-1, F-2)***

R-2. Preclude the use of the AAC algorithm in conjunction with manual steering unless design changes are made to mitigate the adverse interactions (e.g., vehicle's response to pilot commands should not be detected as parasitic dynamics by the AAC spectral damper). ***(F-3, F-4)***

11.0 Alternate Viewpoint

There were no alternate viewpoints identified during the course of this assessment by the NESC team or the NRB quorum.

12.0 Other Deliverables

Several versions of the SLS FCS, SLS reference dynamics, and SLS TC scenarios were delivered from MSFC to AFRC. Following flight tests, AFRC delivered the logged data to MSFC for each flight test scenario as well as the video footage described in Table A-7 in Appendix A. No other unique hardware, software, or data packages, outside those contained in this report, were disseminated to other parties outside this assessment.

13.0 Lessons Learned

The following lessons learned were identified for entry into the NASA Lessons Learned Information System as a result of this assessment:

- The inclusion of a "spectral damper" in the adaptive update law, which has the effect of decreasing the system responsiveness as a result of excitation in the control loop above a prescribed cutoff frequency, is a key contributor to simply, consistently, and predictably mitigating instabilities resulting from unmodeled or mismodeled internal launch vehicle dynamics. This concept may be extensible to other conditionally stable systems.
- The use of NDI allows existing testbeds to mimic the response of a specified dynamic system with an equivalent or slower response. This expands the set of applicable testing options for flight control software. In the case of the SLS AAC system, the F/A-18 was able to provide a cost-effective flight test solution that yielded a large amount of pertinent data.
- The SLS Program, NESC leadership, and Center leadership enabled and encouraged open communications across center and contractor boundaries, and empowered the technical

staff with a high degree of autonomy. The trust given to the LVAC project team by the program leadership contributed to the team's ability to be aggressive and agile, completing all of the milestones on a tight schedule. This high degree of trust from the top was reinforced at the technical level between the partner organizations. This project would not have been the success it was without these relationships founded on trust and mutual respect across all levels of the project team. This relationship was built on and maintained by open and transparent communications regarding all aspects of the project, both positive and negative, without regard for organizational boundaries.

14.0 Recommendations for NASA Standards and Specifications

No recommendations for NASA standards and specifications were identified as a result of this assessment.

15.0 Definition of Terms

Corrective Actions	Changes to design processes, work instructions, workmanship practices, training, inspections, tests, procedures, specifications, drawings, tools, equipment, facilities, resources, or material that result in preventing, minimizing, or limiting the potential for recurrence of a problem.
Finding	A relevant factual conclusion and/or issue that is within the assessment scope and that the team has rigorously based on data from their independent analyses, tests, inspections, and/or reviews of technical documentation.
Lessons Learned	Knowledge, understanding, or conclusive insight gained by experience that may benefit other current or future NASA programs and projects. The experience may be positive, as in a successful test or mission, or negative, as in a mishap or failure.
Observation	A noteworthy fact, issue, and/or risk, which may not be directly within the assessment scope but which could generate a separate issue or concern if addressed. Alternatively, an observation can be a positive acknowledgement of a Center/Program/Project/Organization's operational structure, tools, and/or support provided.
Problem	The subject of the independent technical assessment.
Proximate Cause	The event(s) that occurred, including any condition(s) that existed immediately before the undesired outcome, directly resulted in its occurrence and, if eliminated or modified, would have prevented the undesired outcome.

Recommendation	A proposed measurable stakeholder action directly supported by specific Finding(s) and/or Observation(s) that will correct or mitigate an identified issue or risk.
Root Cause	One of multiple factors (events, conditions, or organizational factors) that contributed to or created the proximate cause and subsequent undesired outcome and, if eliminated or modified, would have prevented the undesired outcome. Typically, multiple root causes contribute to an undesired outcome.
Supporting Narrative	A paragraph, or section, in an NESC final report that provides the detailed explanation of a succinctly worded finding or observation. For example, the logical deduction that led to a finding or observation; descriptions of assumptions, exceptions, clarifications, and boundary conditions. Avoid squeezing all of this information into a finding or observation

16.0 Acronym List

α	Angle of Attack
σ	Standard Deviation
q	Dynamic Pressure
A	"Autopilot" Mode
AAC	Adaptive Augmenting Control
AFRC	Armstrong Flight Research Center (formerly Dryden Flight Research Center)
AMA	Analytical Mechanics Associates
ARI	Attitude Reference Indicator
ARTS	Airborne Research Test System
CDR	Critical Design Review
CxP	Constellation Program
DAC	Design Analysis Cycle
dB	Decibels
DCA	Disturbance Compensation Algorithm
EGI	Embedded GPS INS
F/A	Fighter/Attack
FAST	Full-scale Advanced Systems Testbed
FCS	Flight Control System
FRACTAL	Frequency Response Analysis and Comparison Tool Assuming Linearity
FT	Flight Test
FTP	Flight Test Plan
GN&C	Guidance, Navigation, and Control
GPS	Global Positioning System
GSFC	Goddard Space Flight Center

HILS	Hardware-in-the-Loop Simulation
HUD	Heads-up Display
Hz	Hertz
ILS	Instrument Landing System
INS	Inertial Navigation System
IMU	Inertial Measurement Unit
IRT	Independent Review Team
LaRC	Langley Research Center
LOM	Loss of Mission
LOV	Loss of Vehicle
LSQI	Quadratic Inequality Constrained Least Squares
LVAC	Launch Vehicle Adaptive Control
M	“Manual” Mode
MSFC	Marshall Space Flight Center
MTSO	Management and Technical Support Office
NDI	Nonlinear Dynamic Inversion
NESC	NASA Engineering and Safety Center
NG	Northrop Grumman
NRB	NESC Review Board
ORD	Objectives and Requirements Document
PDR	Preliminary Design Review
PID	Proportional-Integral-Derivative
PIO	Pilot-in-the-Loop Oscillation
PTI	Programmed Test Input
RFA	Request for Action
RFCS	Research Flight Control System
RGA	Rate Gyroscope Assembly
S/L	“Straight and Level” Flight
SIL	Software Integration Laboratory
SLS	Space Launch System
SRB	Solid Rocket Booster
SRDD	Software Requirements and Design Document
STMD	Space Technology Mission Directorate
TC	Test Case
TN	Tail Number
TPM	Technical Performance Metric
TRL	Technology Readiness Level
TVC	Thrust Vector Control
V&V	Verification and Validation
VVTP	Verification and Validation Test Plan

17.0 References

1. Orr, J. and VanZwieten, T.: “Robust, Practical Adaptive Control for Launch Vehicles,” AIAA-2012-4549, August 2012.
2. Hanson, J.: “A Plan for Advanced Guidance and Control Technology for Second Generation Reusable Launch Vehicles,” AIAA-2002-4557, 2002.
3. Wall, J., Orr, J., and VanZwieten, T.: “Space Launch System Implementation of Adaptive Augmenting Control,” in *AAS Guidance, Navigation, and Control Conference Proceedings*, Breckenridge, CO, AAS 14-051, 2014.
4. Orr, J., Wall, J., VanZwieten, T., and Hall, C., “Space Launch System Ascent Flight Control Design,” in *AAS Guidance, Navigation, and Control Conference Proceedings*, Breckenridge, CO, AAS 14-038, 2014.
5. “Control Algorithm and Parameters for the Ares-I-X Flight Test Vehicle,” AI1-SYS-CAP-V4.00, October 2009.
6. Brandon, J., Derry, S., Heim, E., Hueschen, R., and Bacon, B.: “Ares-I-X Stability and Control Flight Test: Analysis and Plans,” in *AIAA Space 2008 Conference Proceedings*, San Diego, CA, 2008.
7. “NASA Research and Technology Program and Project Management Requirements, Appendix J: Technology Readiness Levels (TRLs),” NPR 7120.8, April 18, 2013.
8. Hanson, C.: “Capability Description for NASA’s F/A-18 TN 853 as a Testbed for the Integrated Resilient Aircraft Control Project,” Tech. Rep. DFRC-IRAC-CAP-002, NASA Dryden Flight Research Center, January 2009.
9. Miller, C.: “Nonlinear Dynamic Inversion Baseline Control Law: Architecture and Performance Predictions,” in *AIAA Guidance, Navigation, and Control Conference Proceedings*, Portland, OR, 2011.
10. Miller, C.: “Nonlinear Dynamic Inversion Baseline Control Law: Flight-Test Results for the Full-scale Advanced Systems Testbed F/A-18 Airplane,” in *AIAA Guidance, Navigation, and Control Conference Proceedings*, Portland, OR, 2011.
11. Orr, J., Johnson, M., Wetherbee, J., and McDuffie, J.: “State Space Implementation of Linear Perturbation Dynamics Equations for Flexible Launch Vehicles,” AIAA-2009-5962, 2009.
12. Frosch, J. and Vallely, D.: “Saturn AS-501/S-IC Flight Control System Design,” *J. Spacecraft*, Vol. 4, No. 8, 1967, pp. 1003–1009.
13. Orr, J.: “Elastic Model Transitions Using Quadratic Inequality Constrained Least Squares,” AIAA 2012-4561, August 2012.

14. Jurenko, R., Bush, J., and Ottander, J.: "Elastic Model Transitions: A Hybrid Approach Using Quadratic Inequality Constrained Least Squares (LSQI) and Direct Shape Mapping (DSM)," in *AAS Guidance, Navigation, and Control Conference Proceedings*, AAS 14-034, January/February 2014.
15. Orr, J., Johnson, M., Wetherbee, J., and McDuffie, J.: "State Space Implementation of Linear Perturbation Dynamics Equations for Flexible Launch Vehicles," AIAA 2009-5962, August 2009.
16. Orr, J.: "FRACTAL Linear Model Dynamics," BD TCD20090535A, NASA MSFC/EV41, April 2009.
17. Orr et al. FCS 2014
18. Klein, V. and Morelli, E. A.: *Aircraft System Identification: Theory and Practice*, AIAA Education Series, 2006.
19. Orr, J.: "Optimal Recursive Digital Filters for Active Bending Stabilization," in *AAS Guidance, Navigation, and Control Conference Proceedings*, Breckenridge, CO, 2013.
20. McRuer and Krendel, *Mathematical Models of Human Pilot Behavior*, AGARDograph No. 188, January 1974.
21. Thompson, M. O. and Welsh, J. R.: "Flight Test Experience with Adaptive Control Systems," Advanced Control System Concepts, AGARD CP No. 58, *AGARD Joint Symposium of the Guidance and Control Panel, and the Flight Mechanics Panel of AGARD*, Oslo, Norway, 3–5 September 1968, pp. 141–147, 1970.
22. Bosworth, J. T. and Williams-Hayes, P. S.: "Flight Test Results from the NF-15B Intelligent Flight Control System Project with Adaptation to a Simulated Stabilator Failure," AIAA 2007-2818, 2007.
23. Hanson, C., Schafer, J., Burken, J. J., Johnson, M., and Nguyen, N.: "Handling Qualities Evaluations of Low Complexity Model Reference Adaptive Controllers for Reduced Pitch and Roll Damping Scenarios," AIAA 2011-6607, 2011.
24. "Department of Defense Interface Standard: Flying Qualities of Piloted Aircraft," MIL-STD-1797B, pp. 213–214, February 15, 2006.
25. VanZwieten, T., Gilligan, E., Wall, J., Orr, J., Miller, C., and Hanson, C.: "Adaptive Augmenting Control Flight Characterization Experiment on an F/A-18," in AAS Guidance, Navigation, and Control Conference Proceedings, Breckenridge, CO, AAS 14-052, 2014.

18.0 Appendices (separate Volume 2, Parts 1 and 2)

REPORT DOCUMENTATION PAGE

Form Approved OMB No. 0704-0188

1. REPORT DATE *(DD-MM-YYYY)*: 01- 09 - 2014

2. REPORT TYPE: Technical Memorandum

3. DATES COVERED *(From - To)*: January 2013 - July 2014

4. TITLE AND SUBTITLE
Flight Testing of the Space Launch System (SLS) Adaptive Augmenting Control (AAC) Algorithm on an F/A-18

5a. CONTRACT NUMBER

5b. GRANT NUMBER

5c. PROGRAM ELEMENT NUMBER

6. AUTHOR(S)
Dennehy, Cornelius J.; VanZwieten, Tannen S.; Hanson, Curtis E.; Wall, John H.; Miller, Chris J.; Gilligan, Eric T.; Orr, Jeb S.

5d. PROJECT NUMBER

5e. TASK NUMBER

5f. WORK UNIT NUMBER
869021.05.07.09.27

7. PERFORMING ORGANIZATION NAME(S) AND ADDRESS(ES)
NASA Langley Research Center
Hampton, VA 23681-2199

8. PERFORMING ORGANIZATION REPORT NUMBER
L-20474 NESC-RP-13-00847

9. SPONSORING/MONITORING AGENCY NAME(S) AND ADDRESS(ES)
National Aeronautics and Space Administration
Washington, DC 20546-0001

10. SPONSOR/MONITOR'S ACRONYM(S)
NASA

11. SPONSOR/MONITOR'S REPORT NUMBER(S)
NASA/TM-2014-218528

12. DISTRIBUTION/AVAILABILITY STATEMENT
Unclassified - Unlimited
Subject Category 15 Launch Vehicles and Launch Operations
Availability: NASA CASI (443) 757-5802

13. SUPPLEMENTARY NOTES

14. ABSTRACT
The Marshall Space Flight Center (MSFC) Flight Mechanics and Analysis Division developed an adaptive augmenting control (AAC) algorithm for launch vehicles that improves robustness and performance on an as-needed basis by adapting a classical control algorithm to unexpected environments or variations in vehicle dynamics. This was baselined as part of the Space Launch System (SLS) flight control system. The NASA Engineering and Safety Center (NESC) was asked to partner with the SLS Program and the Space Technology Mission Directorate (STMD) Game Changing Development Program (GCDP) to flight test the AAC algorithm on a manned aircraft that can achieve a high level of dynamic similarity to a launch vehicle and raise the technology readiness of the algorithm early in the program. This document reports the outcome of the NESC assessment.

15. SUBJECT TERMS
NASA Engineering and Safety Center; Adaptive Augmenting Control; Space Launch System; Guidance, Navigation and Control; F/A-18

16. SECURITY CLASSIFICATION OF: a. REPORT	b. ABSTRACT	c. THIS PAGE	17. LIMITATION OF ABSTRACT	18. NUMBER OF PAGES	19a. NAME OF RESPONSIBLE PERSON
					STI Help Desk (email: help@sti.nasa.gov)
					19b. TELEPHONE NUMBER *(Include area code)*
U	U	U	UU	66	(443) 757-5802

Standard Form 298 (Rev. 8-98)
Prescribed by ANSI Std. Z39.18